

AD-A085 647

TRANSPORTATION SYSTEMS CENTER CAMBRIDGE MA
GROUND WIND VORTEX SENSING SYSTEM CALIBRATION TESTS. (U)
FEB 80 T E SULLIVAN, D C BURNHAM
TSC-FAA-80-4 FAA-RD-80-13

F/G 14/2

UNCLASSIFIED

FAA-RD-80-13

NL

1 OF 1
AD
ADP886-1

END
DATE
FILMED
7-80
DTIC

4

LEVEL

FAA-RD-80-13

GROUND WIND VORTEX SENSING SYSTEM CALIBRATION TESTS

12

ADA 085647

FEBRUARY 1980

DTIC
JUN 16 1980
C

U.S. DEPARTMENT OF TRANSPORTATION

RESEARCH AND SPECIAL PROGRAMS ADMINISTRATION
TRANSPORTATION SYSTEMS CENTER • CAMBRIDGE MA 02142

PREPARED FOR FEDERAL AVIATION ADMINISTRATION
SYSTEMS RESEARCH AND DEVELOPMENT SERVICE • WASHINGTON DC 20590

This document has been approved
for public release and sale; its
distribution is unlimited.

80 6 12 014



DDC FILE COPY

NOTICE

This document is disseminated under the sponsorship of the Department of Transportation in the interest of information exchange. The United States Government assumes no liability for its contents or use thereof.

NOTICE

The United States Government does not endorse products or manufacturers. Trade or manufacturers' names appear herein solely because they are considered essential to the object of this report.

1. Report No. FAA-RD-80-13		2. Government Accession No. AD-A085 647		3. Recipient's Catalog No. (12) 84	
4. Title and Subtitle (6) GROUND WIND VORTEX SENSING SYSTEM CALIBRATION TESTS.		5. Report Date (11) Feb 1980		6. Performing Organization Code (14)	
7. Author(s) (10) T.E./Sullivan, D.C./Burnham		8. Performing Organization Report No. DOT/TSC-FAA-80-4		9. Work Unit No. (TRAIS) FA905/R0132	
10. Performing Organization Name and Address U.S. Department of Transportation Research and Special Programs Administration Transportation Systems Center Cambridge MA 02142		11. Contract or Grant No.		12. Type of Report and Period Covered Final Report Apr 1971 - Nov 1972	
12. Sponsoring Agency Name and Address U.S. Department of Transportation Federal Aviation Administration Systems Research and Development Service Washington DC 20591		13. Sponsoring Agency Code		14. Supplementary Notes	
15. Abstract <p>This report describes the collection of data related to the calibration of two systems for detecting and tracking aircraft wake vortices. The systems tested were the propeller anemometer Ground Wind Vortex Sensing System and the Pulsed Acoustic Vortex Sensing System.</p> <p>The data were analyzed and the location of the vortices as determined with these systems were compared with the vortex location as determined photographically.</p> <p>The tests were conducted at the Federal Aviation Administration's National Aviation Facilities Experimental Center, in Atlantic City, NJ.</p>					
16. Key Words Vortex Sensing Tests, Acoustic Sensors, Wind Sensors, Aircraft Wake Vortices		17. Distribution Statement DOCUMENT IS AVAILABLE TO THE PUBLIC THROUGH THE NATIONAL TECHNICAL INFORMATION SERVICE, SPRINGFIELD, VIRGINIA 22161			
18. Security Classif. (of this report) Unclassified		19. Security Classif. (of this page) Unclassified		20. No. of Pages 88	
21. Price					

PREFACE

In the spring and fall of 1972, the Transportation Systems Center (TSC), in collaboration with the National Aviation Facilities Experimental Center (NAFEC), tested the accuracy of various systems for detecting and tracking wake vortices. The tests demonstrated the feasibility of the propeller anemometer ground wind vortex sensing system (GWVSS) and the pulsed acoustic vortex (PAVSS).

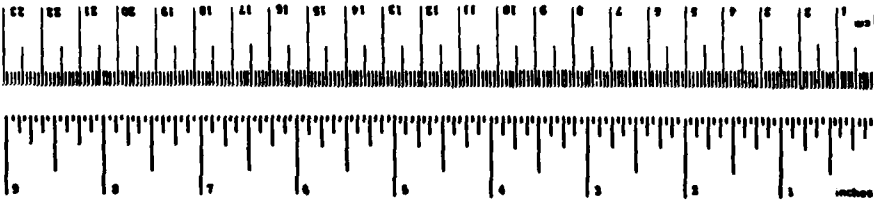
No final report was written on these tests because other projects in the wake vortex program had higher priority. Analysis of data collected over the past few years by the GWVSS has resulted in the installation of the Vortex Advisory System at O'Hare International Airport in Chicago, Illinois. This system advises the air traffic controller of the conditions under which interarrival aircraft separation can be reduced to a uniform 3 nautical miles. The main purpose of this report is to provide a calibration of the GWVSS.

Accession For	
NTIS	DTIC
DDC TAB	
Unannounced	
Justification	
By	
Distribution/	
Availability Codes	
Dist	Avail and/or special
A	

METRIC CONVERSION FACTORS

Approximate Conversions to Metric Measures

Symbol	When You Know	Multiply by	To Find	Symbol
LENGTH				
in	inches	2.5	centimeters	cm
ft	feet	30	meters	m
y	yards	0.9	meters	m
m	miles	1.6	kilometers	km
AREA				
sq in	square inches	6.5	square centimeters	sq cm
sq ft	square feet	0.09	square meters	sq m
sq yd	square yards	0.8	square meters	sq m
sq mi	square miles	2.6	square kilometers	sq km
ac	acres	0.4	hectares	ha
MASS (weight)				
oz	ounces	28	grams	g
lb	pounds	0.45	kilograms	kg
short ton	short tons (2000 lb)	0.9	metric tons	t
VOLUME				
teaspoon	teaspoons	5	milliliters	ml
tablespoon	tablespoons	15	milliliters	ml
fluid ounce	fluid ounces	30	milliliters	ml
cup	cups	0.24	liters	l
pint	pints	0.47	liters	l
quart	quarts	0.95	liters	l
gallon	gallons	3.8	liters	l
cubic foot	cubic feet	0.03	cubic meters	m ³
cubic yard	cubic yards	0.76	cubic meters	m ³
TEMPERATURE (exact)				
Fahrenheit temperature	5/9 (after subtracting 32)		Celsius temperature	°C



Symbol	When You Know	Multiply by	To Find	Symbol
LENGTH				
mm	millimeters	0.04	inches	in
cm	centimeters	0.4	inches	in
m	meters	1.1	yards	yd
km	kilometers	0.6	miles	mi
AREA				
sq cm	square centimeters	0.16	square inches	sq in
sq m	square meters	1.2	square yards	sq yd
sq km	square kilometers	0.4	square miles	sq mi
ha	hectares (10,000 m ²)	2.5	acres	ac
MASS (weight)				
g	grams	0.005	ounces	oz
kg	kilograms	2.2	pounds	lb
metric ton	metric tons (1000 kg)	1.1	short tons	short ton
VOLUME				
ml	milliliters	0.05	fluid ounces	fl oz
l	liters	1.06	quarts	qt
l	liters	0.26	gallons	gal
m ³	cubic meters	36	cubic feet	cu ft
m ³	cubic meters	1.3	cubic yards	cu yd
TEMPERATURE (exact)				
°C	Celsius temperature	9/5 (then add 32)	Fahrenheit temperature	°F

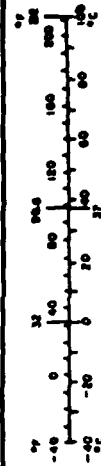


TABLE OF CONTENTS

<u>Section</u>	<u>Page</u>
1. INTRODUCTION.....	1
2. DESCRIPTION OF THE TESTS.....	2
2.1 Test Configurations.....	2
2.2 Pulsed Acoustic System.....	7
2.3 Ground Wind Tracking System.....	10
2.3.1 Pressure Sensors.....	10
2.3.2 Propeller Anemometers.....	14
2.4 Aircraft Detectors.....	17
2.5 Photographic System.....	17
2.6 NAFEC Participation.....	24
3. TEST RESULTS.....	26
Data Analysis.....	26
4. DISCUSSION.....	67
4.1 Acoustic Sensors.....	67
4.2 Ground Wind Sensors.....	67
4.3 Aircraft Detector.....	68
5. CONCLUSIONS.....	71
6. REFERENCES.....	75
APPENDIX -- Analysis of Photographic Tracking Data.....	77

LIST OF ILLUSTRATIONS

<u>Figure</u>		<u>Page</u>
1.	Sensors Installed at +350 Ft on the 040°-220° Baseline.....	3
2.	Map of Test Area Showing the Baselines and Camera Sites for the Second Series of Tests.....	5
3.	Flight Paths vs. Wind Direction for the Second Series of Tests.....	6
4.	Acoustic Speaker Positions.....	8
5.	Acoustic Speaker and Antenna Positioned at Ground Level.....	9
6.	Sensor Locations for the First Series of Tests..	11
7.	Sensor Locations for the Second Series of Tests.	11
8.	Boeing 727 Aircraft over Post with Propeller Anemometer and 180° Dual Pilot Tube.....	15
9.	Propeller Anemometers (a) Four-Blade, (b) De Facto Two-Blade.....	16
10.	Aircraft Detector.....	18
11.	Vortex Axis Due to Aircraft Crabbing.....	21
12.	Typical Sequence of Tracking Photographs.....	22
13.	Propeller Anemometer Data, 9/14/72, B-727 Air- craft. Aircraft Altitude = 130', Aircraft Lateral Position = -150'.....	29
14.	Propeller Anemometer Data, 9/17/72, B-747 Air- craft. Aircraft Altitude = 150', Aircraft Lateral Position = -200'.....	30
15.	Comparison of Pressure Sensor and Propeller Anemometer Data of Runs 747-28, 29.....	31
16.	Comparison of Pressure Sensor and Propeller Anemometer Data of Runs 747-30, 31.....	32
17.	Vortex Tracks from Propeller Anemometer Data....	33
18.	Tape Recorder Channel Use with Data of Run 747-26.....	33

LIST OF ILLUSTRATIONS (CONT'D)

<u>Figure</u>		<u>Page</u>
19.	Aircraft Detector Data.....	34
20.	Computer Produced Acoustograms.....	36
21.	Computer Produced Vortex Tracks.....	37
22.	NAFEC Tower Tests, 9/15/72, Run 727-178 Downwind Vortex.....	40
23.	NAFEC Tower Tests, 9/15/72, Run 727-180 Downwind Vortex.....	42
24.	NAFEC Tower Tests, 9/15/72, Run 727-181 Downwind Vortex.....	44
25.	NAFEC Tower Tests, 9/15/72, Run 727-182 Downwind Vortex.....	46
26.	NAFEC Tower Tests, 9/17/72, Run 747-42 Downwind Vortex.....	48
27.	NAFEC Tower Tests, 9/17/72, Run 747-42 Upwind Vortex.....	50
28.	NAFEC Tower Tests, 9/17/72, Run 747-43 Downwind Vortex.....	52
29.	NAFEC Tower Tests, 9/17/72, Run 747-43 Upwind Vortex.....	54
30.	NAFEC Tower Tests, 9/17/72, Run 747-44 Downwind Vortex.....	56
31.	NAFEC Tower Tests, 9/17/72, Run 747-44 Upwind Vortex.....	58
32.	NAFEC Tower Tests, 9/17/72, Run 747-45 Downwind Vortex.....	60
33.	NAFEC Tower Tests, 9/17/72, Run 747-45 Upwind Vortex.....	62
34.	NAFEC Tower Tests, 9/17/72, Run 747-48 Downwind Vortex.....	64
A1.	Geometrical Analysis of Vortex Location.....	78

LIST OF TABLES

<u>Table</u>		<u>Page</u>
1.	TEST SERIES ONE GROUND WIND SENSOR LOCATIONS...	12
2.	TEST SERIES TWO GROUND WIND SENSOR LOCATIONS...	13
3.	CAMERA SITES.....	19
4.	LIST OF NAFEC TESTS.....	27
5.	FIGURE NUMBERS FOR VORTEX TRAJECTORY PLOTS.....	66

1. INTRODUCTION

The TSC development of pulsed acoustic and ground wind vortex tracking systems is described in three earlier reports ¹⁻³. With the exception of a short series of tests at NAFEC during June and July of 1971, the targets used in the sensor development were vortices produced by aircraft making normal runway approaches at airports. Although experiments carried out in this manner have the virtue of testing a sensor in an operational environment, they have a number of drawbacks which hinder a full understanding of sensor capabilities. These limitations in descending order of importance are:

- a) The nature and location of the vortices are not precisely known and therefore no check on system accuracy is possible.
- b) The range of aircraft altitudes at a particular site is very limited.
- c) Only one configuration of the aircraft can be studied.

In order to determine the accuracy with which a tracking system can locate a vortex, some independent method of vortex location is required. The first effort in this direction used the NAFEC-instrumented tower to obtain a single calibration point.

The vortex arrival time and height at the tower were determined by hot wire anemometers and were compared to the vortex tracks obtained by a first-generation pulsed acoustic system. However, point calibration proved to be an inefficient way of calibrating any tracking system, especially since the sensitivity and accuracy of this tracking system is a strong function of vortex position. During the July 1971 C-5A NAFEC tower tests, it was observed that a vortex passing through the NAFEC tower can be tracked for a considerable distance past the tower by photographing the smoke used for flow visualization at the tower. This technique was used in the majority of the tests reported here.

2. DESCRIPTION OF THE TESTS

The first series of tests took place in April and May of 1972 using the following aircraft types: the C-5A, the C-141, the DC-7, and the CV-880. Since these tests were scheduled for the calibration of the Xonics acoustic sensor, no additional acoustic equipment could be deployed because of possible interference. The TSC testing was limited to tracking the vortices by timed photography and ground level pressure sensors.

The second series of tests took place from August to November 1972. They were scheduled a week at a time with two or three week intervals for data analysis. The following aircraft were used: The DC-6 (NAFEC), the CV-880 (NAFEC), the B-727 (FAA, Oklahoma), the B-727 (United Airlines), the B-747 (Pan Am) and the B-707 (Pan Am). In addition to the two TSC sensors, the TSC photographic tracking, and the NAFEC meteorological sensors, all described above, several other measurements were made to take advantage of the presence of vortices under controlled conditions. The NAFEC tower hot-wire anemometers were operated during the B-727, B-747 and B-707 Tests. During a portion of this test series, a group from the Massachusetts Institute of Technology, under contract to TSC, studied the acoustic back scattering properties of aircraft vortices.

2.1 TEST CONFIGURATIONS

The basic goal of these calibration tests was to determine how effectively certain sensing systems could track vortices in a plane roughly perpendicular to the aircraft flight path. All sensing systems were installed on the same baseline (Figure 1), and the absolute vortex locations were measured by photographing smoke from the NAFEC instrumented tower. The aircraft flight path was approximately perpendicular to the ambient wind for good smoke visualization. It was decided that this requirement would be satisfied best by instrumenting two complete sensor baselines. This would provide reasonable coverage for any wind conditions and would not require an excessive amount of equipment or set-up time.



FIGURE 1. SENSORS INSTALLED AT +350 FT ON THE 040°-220° BASELINE. The Speaker is #17 in Figure 4.

The tests were carried out in the vicinity of the NAFEC tower. (See Figure 2.) The location of the two baselines was subject to two restrictions: a) The aircraft flight path had to be at a safe distance from both the 140-foot smoke tower and the much larger 160-foot meteorological tower located 500 feet to the northeast. b) The sensor baselines and the camera sites had to lie on NAFEC property which is limited in certain directions. In both test series, one baseline was chosen to lie on a heading of 040° - 220° magnetic since NAFEC records showed that the prevailing wind was from the southwest during previous vortex tests. Moreover, this orientation allows the maximum possible air space for aircraft flying between the two towers. The selection of the second baseline was more difficult. In the first test series, it was oriented at 090° - 270° (Figure 6 in Section 3) so that it would be perpendicular to a northerly flight path, giving safe clearance of the meteorological tower for flights close to the instrumented tower.

In the second test series (Figure 2), the second baseline was chosen to be perpendicular to the first at a heading of 130° - 310° . It was then possible to select a set of sensors so that the angle between the wind and the sensor baseline never exceeded 45° . Both baselines were located 50' from the tower to minimize reflections. With these two baselines, the required aircraft path as a function of ambient wind is shown in Figure 3. The aircraft heading was always toward the camera site. (This requirement is discussed in Sections 2.5 and 3.2.3). The aircraft flight paths for winds in quadrants 2 and 4 are relatively free of obstructions. However, the remaining two are limited. When the wind is in quadrant #1, the flight paths for the larger aircraft can be no less than 300' from the smoke tower because of the hazard presented by the meteorological tower. When the wind is in quadrant #3, the flight path lies between the two towers, which are only 500' apart. This path requires precise positioning of the aircraft, particularly when the aircraft altitude is low (<200').

The camera sites were chosen to be as far from the tower as possible and yet to remain at a high enough elevation to include

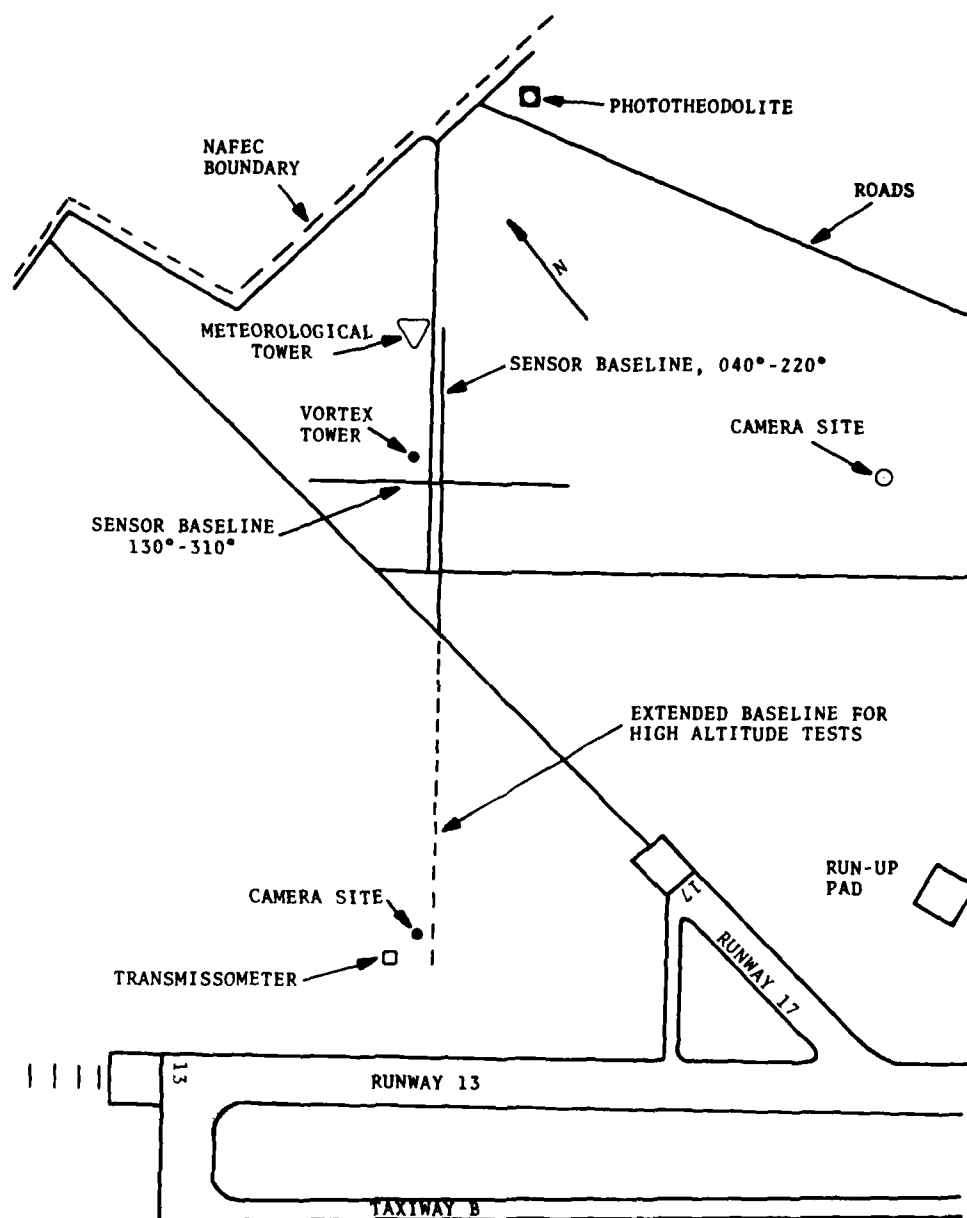


FIGURE 2. MAP OF TEST AREA SHOWING THE BASELINES AND CAMERA SITES FOR THE SECOND SERIES OF TESTS

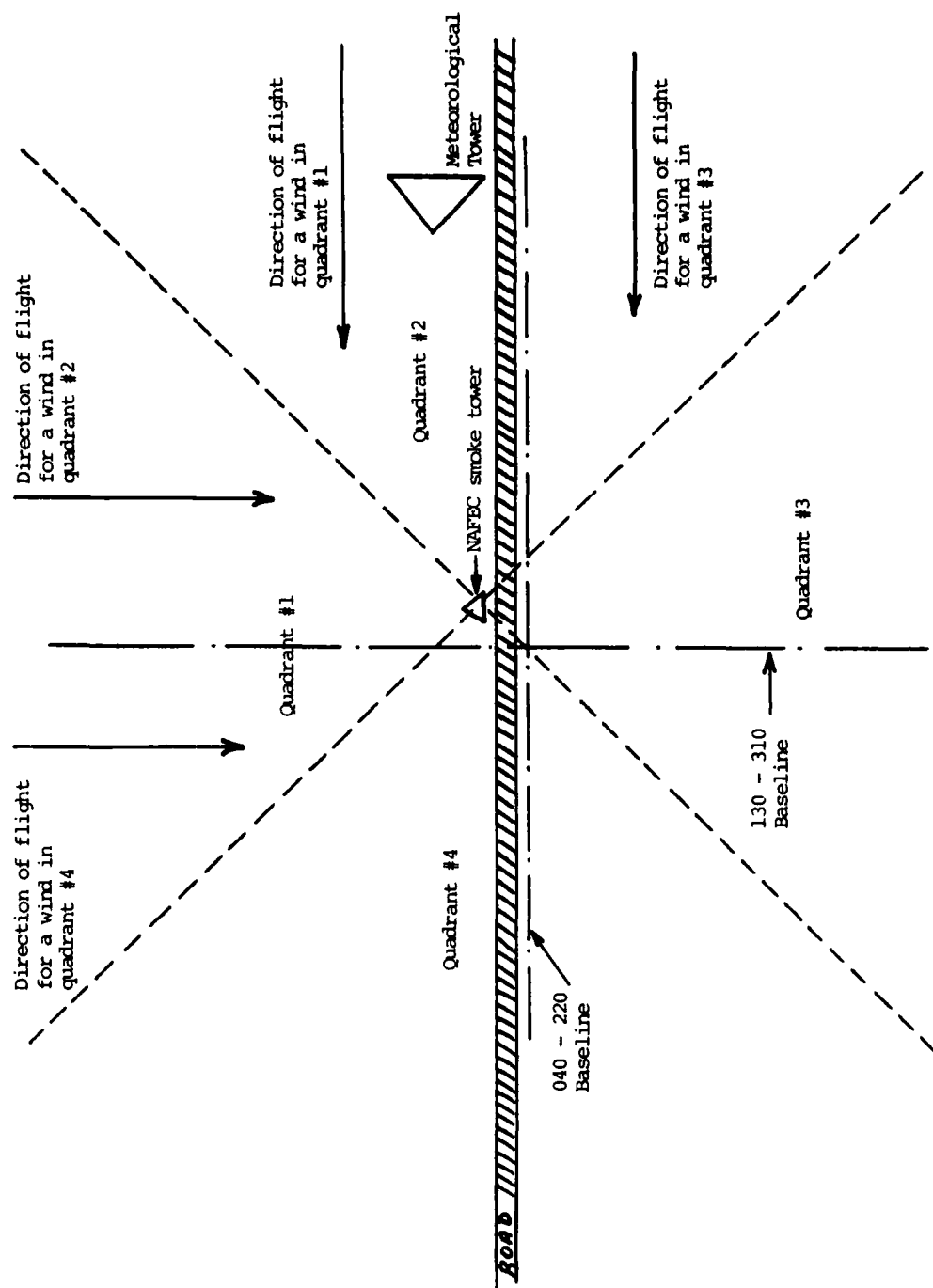


FIGURE 3. FLIGHT PATHS VS. WIND DIRECTION FOR THE SECOND SERIES OF TESTS

the reference signs in the field of view. The signs consisted of 2' x 2.5' sections of pressboard painted with a white background and a dark numeral indicating the distance from the tower in hundreds of feet. They were mounted on metal posts approximately 4' or 5' high. (See Figure 1.)

The positions of all sensors and sign posts were accurately surveyed using a transit and 100' tape measure.

2.2 PULSED ACOUSTIC SYSTEM

The acoustic sensing system electronics, acoustic transducers, and supports were essentially the same as those used in tests at Kennedy Airport (Ref. 3).

The spacing between transceivers was reduced from 330 feet (used in the Kennedy tests) to 165 feet. (See Figure 4.) This change increased the inherent system accuracy for vortices relatively close to the tower, and insured that vortices which passed through the tower would have a scattering angle less than one radian for a sufficient number of transceiver combinations to obtain a vortex track. One drawback of this arrangement is that vortices can only be tracked over relatively short distances (+500' maximum).

One transceiver was positioned on the 040°-220° baseline at a distance of 2064' from the tower and was used with transceivers #15 and #18 in the high altitude tests. The aircraft flight path was 400' to 1000' southwest of the tower at a heading of 130° or 310° and at altitudes ranging from 300' to 900'.

The salient features of the PAVSS were:

- a) The pulse repetition period was 450 msec. (nominal)
- b) The pulse width was 3 msec. (nominal)
- c) Stations numbered 11, 12, 17, 18, 21, 22, 27 and 28 were elevated to a height of 8 feet to improve the ground pulse signal.

An example of a typical PAVSS sensor is shown in Figure 5.

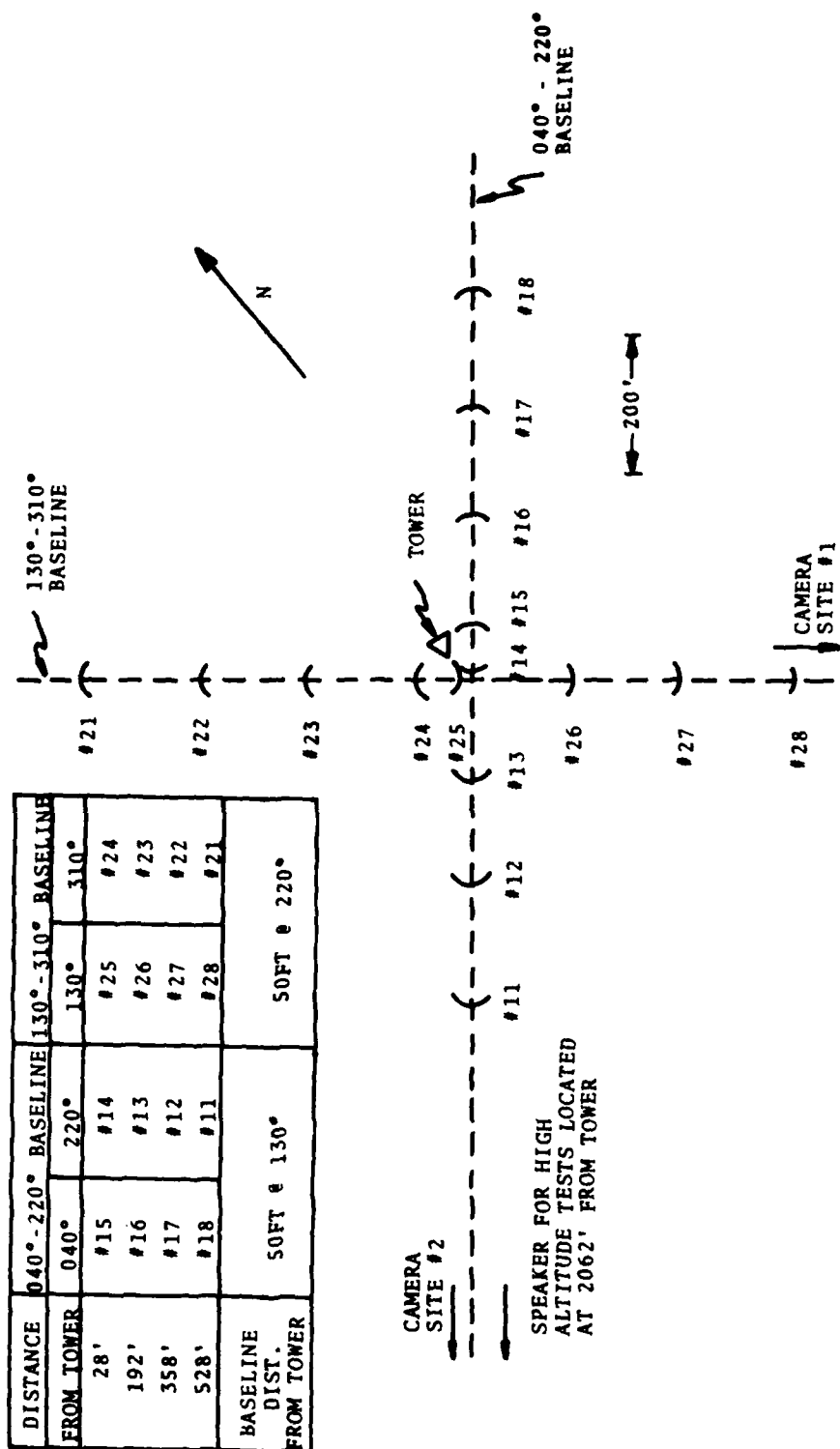


FIGURE 4. ACOUSTIC SPEAKER POSITIONS

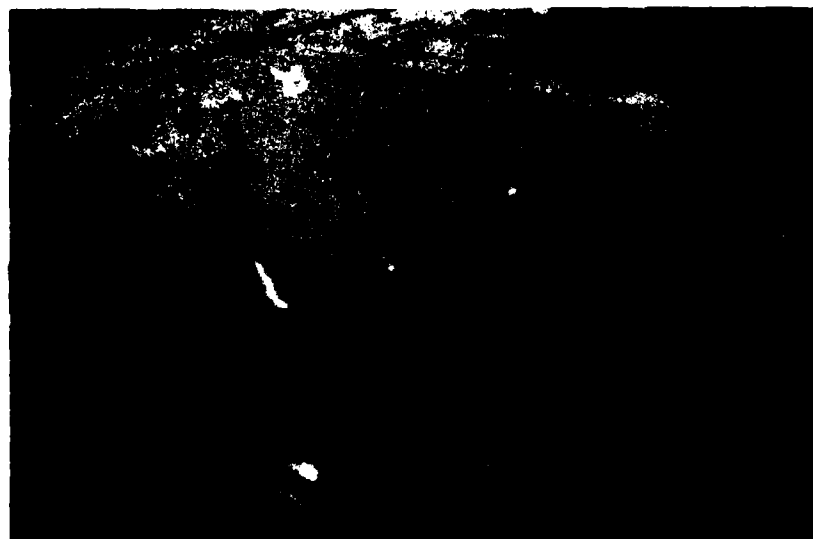


FIGURE 5. ACOUSTIC SPEAKER AND ANTENNA POSITIONED AT GROUND LEVEL

2.3 GROUND WIND TRACKING SYSTEM

The sensor locations for the two series of tests are shown in Figures 6 and 7 and Tables 1 and 2. In many cases, several sensors were installed at the same location in order to make direct comparisons of the signals from different sensors.

The proper sensor spacing in an array is a compromise between the resolution desired and the number of sensors needed to cover the required space. Since the 200-ft spacing used in the earlier tests at Kennedy Airport³ was felt to be inadequate for reliable tracking, 100-ft spacing was used in these tests.

In the first series of tests the ground wind data were collected from up to 12 sensors and were recorded on 2 7-channel Ampex SP-300 tape recorders (6 fm data channels and 1 comment channel each). In the second series, the data from up to 24 sensors were recorded on an Ampex SP-700 tape recorder (1 comment channel, 2 fm channels and 30 time-shared channels with 0-5 Hz bandwidth). In all tests 8 channels of data were recorded in real time on a Brush 816 strip chart recorder.

2.3.1 Pressure Sensors

The function of a ground wind sensor, as described in an earlier report³, is to measure the component of the wind at ground level perpendicular to the aircraft path.

The 120° Dual Pitot tube pressure sensor was designed to detect this wind component in the presence of a larger wind component parallel to the aircraft path, as is encountered in normal airport operations. However, the tests at NAFEC were conducted with the aircraft path perpendicular to the ambient wind and, therefore, with little or no parallel wind component. Consequently, the dual Pitot tubes (the locations of which are indicated by the suffix D in Table I) were oriented at 180° for these tests, both tubes being perpendicular to the aircraft flight path. For comparison purposes, during the first series of tests some sensor locations were instrumented with three tubes (the locations of which

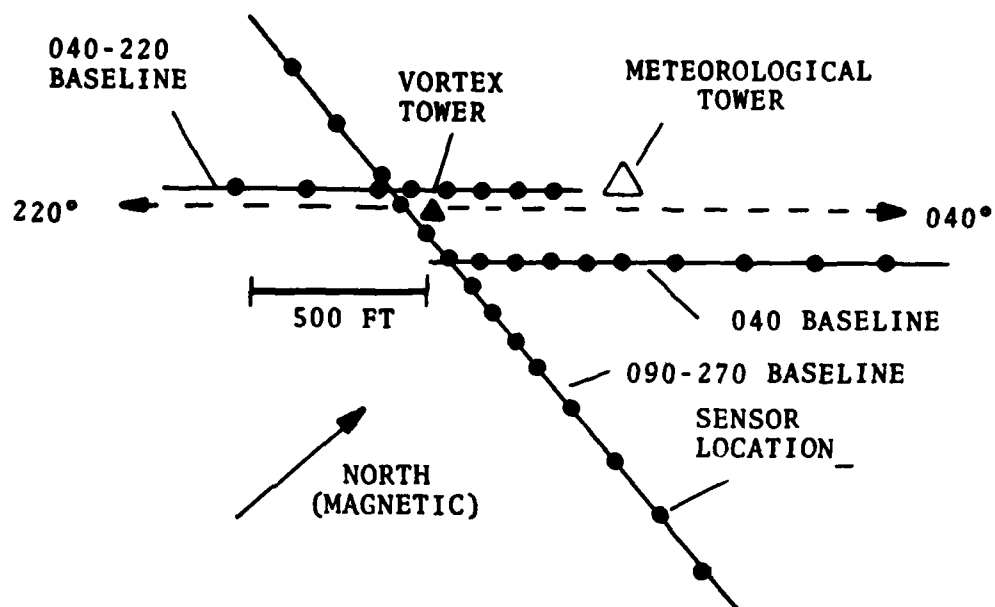


FIGURE 6. SENSOR LOCATIONS FOR THE FIRST SERIES OF TESTS

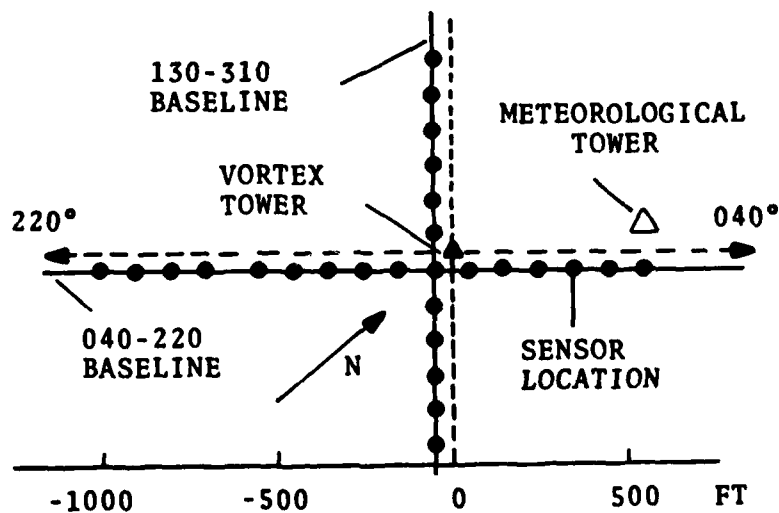


FIGURE 7. SENSOR LOCATIONS FOR THE SECOND SERIES OF TESTS

TABLE 1. TEST SERIES ONE GROUND WIND SENSOR LOCATIONS

Distance	Sensor Elevation and Type				
	040°-220°	Baseline	040° Baseline	90°-270°	Baseline
	040°	220°	040°	90°	270°
50 ft.	5T,12T*	5D	5D	5D	5D
150	5D**	5T,12T	5D	5T,12T	5D
250	5T		5D	5D	
350	5D	5T	5D	5D	5D
450			5D	5D	
550		5T	5D	5D	5D
700			5D	5D	
900			5D	5D	
1100			5D	5D	
1300			5D	5D	
Baseline Distance from Tower	50 ft. @ 310°		150 ft. @ 130°	50 ft. @ 180°	

*Suffix T indicates co-location of a three-component Pitot tube.

**Suffix D indicates co-location of a two-component Pitot Tube.

TABLE 2. TEST SERIES TWO GROUND WIND SENSOR LOCATIONS

Distance	Number of Cables			
	040°-220° Baseline		130°-310° Baseline	
	040°	220°	130°	310°
50 ft.	1	1	1	1
150	2	2	2	2
250	2	1	1	1
350	1	2	2	2
450	1	1	1	1
550	1	1	1	1
700	0	1	0	0
800	0	1	0	0
900	0	1	0	0
1000	0	1	0	0
Baseline Distance from Tower	50 ft. @ 130°		48 ft. @ 220°	

Sensor elevation = 6 1/2 ft.

are indicated by the suffix T in Table 1) two pointing horizontally at 180° and one pointing vertically.

In the first series of tests, it was found that the pressure sensors did not perform as well as they had in previous airport tests. Also, the signal response was much larger from the first vortex than from the second. (See Section 4.2.) These difficulties led to the consideration of the propeller anemometer as a more reliable vortex sensor.

2.3.2 Propeller Anemometers

A sensor having a linear response to the wind velocity and a stable zero level has the following advantages over pressure sensors for detecting and tracking aircraft vortices:

- a) A quantitative measurement of the vortex winds is possible. (Reference 3 describes the deficiencies of pressure sensors in this respect.)
- b) The sensitivity of the sensor is the same for both vortices under all ambient wind conditions.
- c) Real time tracking, which requires a comparison of simultaneous wind measurements at various locations, is more practical.

A survey of the field showed that the most economical sensor having a linear response and a stable zero is a propeller anemometer driving a dc generator. The possible drawbacks compared to a pressure sensor are poor speed of response and reduced reliability because of delicate moving parts. Fixed-axis Gill propeller anemometers, manufactured by the R.M. Young Company, were used in the second test series. (See Figure 8.) Their response distance is 3 ft and threshold speed 0.4 MPH. These specifications appear to be more than adequate for vortex tracking. The first propellers used styrofoam and were fragile and easily broken by careless handling. When one of the four blades was broken, the opposing blade was trimmed to restore balance. (See Figure 9.) By the end of the tests, about half of the propellers had



FIGURE 8. BOEING 727 AIRCRAFT OVER POST WITH PROPELLER ANEMOMETER AND 180° DUAL PILOT TUBE



(a)



(b)

FIGURE 9. PROPELLER ANEMOMETERS
(a) FOUR-BLADE
(b) DE FACTO TWO-BLADE

become two-bladed, with all but one due to careless handling. The major operational difficulty with the propeller anemometers occurred when rain was followed by freezing temperatures. Water which entered the propeller shaft bearing turned to ice and stopped the propeller from turning. The manufacturer recommends that air be blown continually through this bearing when the shaft is mounted horizontally or a small heater be used to eliminate this problem.

2.4 AIRCRAFT DETECTORS

From earlier studies^{2,3}, it was known that a pressure sensor can detect the pressure wave associated with an aircraft passing over it. During these tests pressure sensors were deployed to obtain quantitative data on the amplitude and duration of the pressure signals as a function of aircraft type, altitude and lateral offset. The aircraft detectors used a differential pressure sensor to compare the instantaneous ambient pressure with the average ambient pressure, contained in a vessel with a slow leak (a hypodermic needle) to the atmosphere. The time constant for the reference vessel was set at 20-40 sec but sometimes became less because of additional leaks. The first aircraft detectors used a glass flask as the reference vessel and suffered from drastic instabilities on sunny days. This problem was overcome when, following the suggestion of NAFEC personnel, dewar flasks were used for the reference vessel. The aircraft detectors were placed on the ground with the open port of the differential pressure sensor pointed vertically. (See Figure 10.)

2.5 PHOTOGRAPHIC SYSTEM

The photographic system was used to measure the initial aircraft position and track vortices which pass through the smoke tower. The photographs were taken from a relatively distant point so that the vortex is viewed approximately down the core for long tracking distances.

The camera sites selected are listed in Table 3; those for the second series of tests are shown in Figure 2. The direction of the sites from the tower was based on available land and the

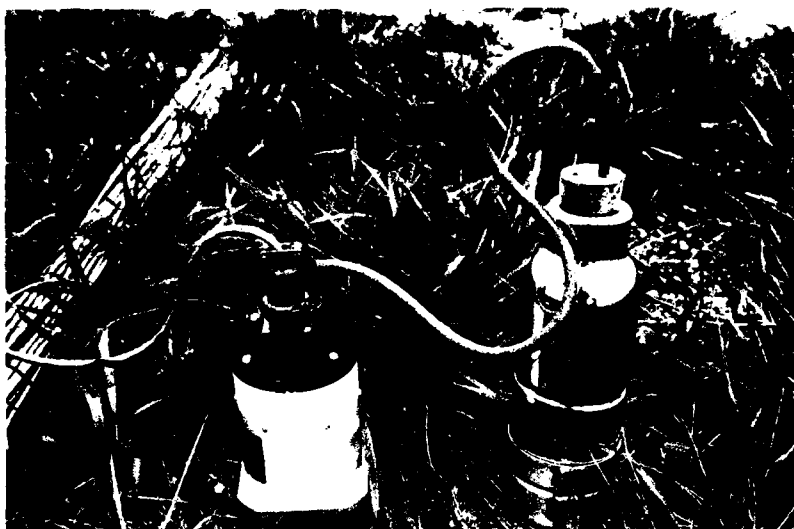


FIGURE 10. AIRCRAFT DETECTOR

TABLE 3. CAMERA SITES

Baseline	Tower Distance	Direction (magnetic)	Baseline Coordinates (see Appendix)	
----------	----------------	-------------------------	--	--

Series One

L

D

040°-220°	1901 ft.	123.02°	1887 ft.	231 ft.
090°-270°	1365 ft.	176.25°	1362 ft.	89 ft.

Series Two

040°-220°	1777 ft.	129.78°	1777 ft.	7 ft.
130°-310°	2042 ft.	219.97°	2042 ft.	1 ft.

position of the sun during the morning tests. The detailed locations were chosen to insure that the vortex could be viewed directly down the core for aircraft flying perpendicular to the baseline. This requirement is discussed in greater detail in Section 3.2.3.

In the first series of tests, the camera sites were chosen to be perpendicular to the baseline somewhat downwind from the tower, so that the optimal view of the vortex would occur after the vortex passed the tower. This procedure would require four camera sites to account for all wind directions. In the second test series, the same effect was achieved with only two camera sites by making careful use of aircraft crabbing. The aircraft were guided on a particular path by means of three strobe lights at ground level spaced along a line perpendicular to the sensor baseline. Because of the crosswind, the aircraft heading and, hence, the vortex axis are slightly tilted with respect to the flight path set by the strobes. If the aircraft is flying toward a camera site which is located perpendicular to the baseline at the tower, the tilt will cause the vortex to line up with the camera view somewhat after passing through the tower. (See Figure 11.) The same result is obtained for parallel flight paths on either side of the tower. This choice of flight direction caused some difficulties for the pilots since they had to approach the test area from a wooded area.

The picture-taking sequence consisted of a single photograph taken as the aircraft passed the tower and a sequence of evenly timed (1-4 second intervals) photographs beginning at a set time (typically 20-50 seconds) after aircraft passage and ending when the vortices could no longer be seen in the smoke. A typical example is given in Figure 12. The photograph of the aircraft can be analyzed by scaling and trigonometric techniques (as in previous tests³) to determine the aircraft position abreast of the smoke tower, and hence the initial vortex locations. A relatively long time delay elapses before the next photograph since the vortices are not visualized until they reach the smoke tower. Photographs of the visualized vortices are then taken at relatively short intervals until the vortices are no longer visible.

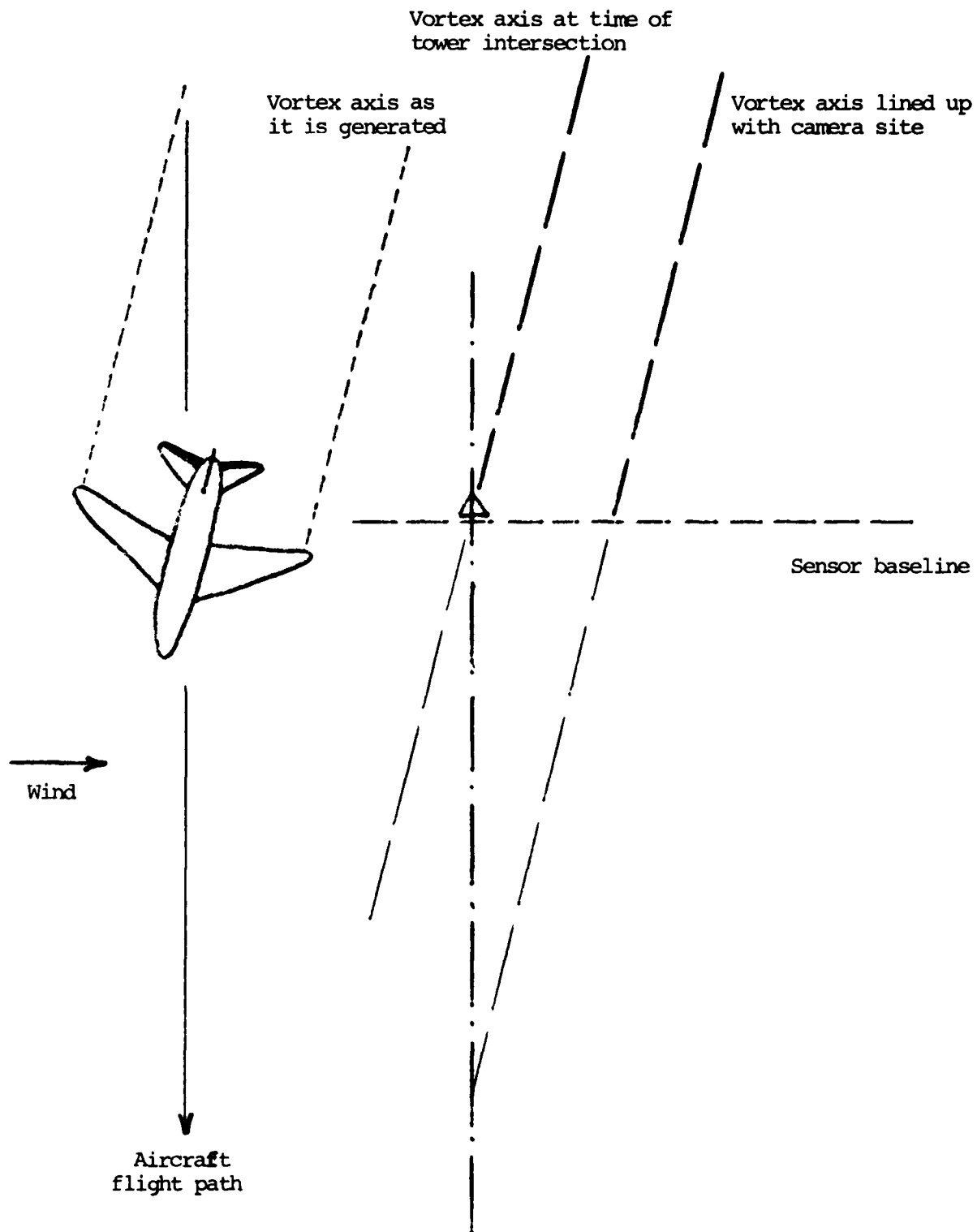
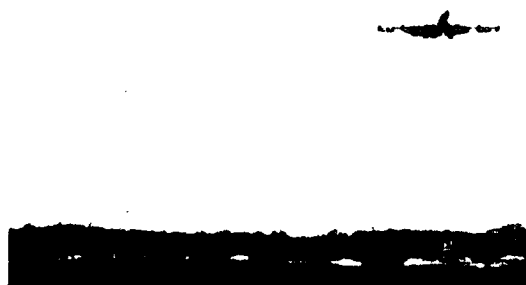


FIGURE 11. VORTEX AXIS DUE TO AIRCRAFT CRABBING



$t = 0 \text{ sec.}$



$t = 21 \text{ sec.}$



$t = 39 \text{ sec.}$



$t = 48 \text{ sec.}$



$t = 57 \text{ sec.}$



$t = 66 \text{ sec.}$

FIGURE 12. TYPICAL SEQUENCE OF TRACKING PHOTOGRAPHS

This interval is selected to obtain a reasonable vortex track under the given conditions.

In the early tests several different film types were tested (viz., Ektachrome MS, High Speed Ektachrome, Kodachrome X, Kodachrome II, Kodacolor and SO 456). After several rolls of each type were evaluated, Kodachrome II was selected because it gave the best combination of film speed and color intensity. In special situations (e.g., very low light levels) other films were used as needed. The primary photographic system consisted of a NIKON F 35mm single lens reflex camera with a 50-300mm f/4.5 zoom lens and a motorized back which accepts 250 exposure cartridges.

The picture-taking sequence was controlled by a custom-built timing circuit with an internal 100 KHz crystal clock and integrated circuit logic. The two inputs to this circuit are a start-of-run signal and an end-of-run signal. In the first series of tests, the start-of-run was initiated manually by monitoring a flash bulb at the base of the tower which was ignited by the NAFEC start-of-run signal. This procedure had three disadvantages: a) At times the observer would miss this flash, and as a result the photographic data would not be synchronized with that of the NAFEC and TSC sensor data, which were mutually synchronized by means of a cable; b) The response time of the observer introduces some uncertainty into the synchronization; c) The ignition of the flashbulb was sometimes unreliable. In the second series of tests, an electronic start-of-run signal was supplied to both camera sites, and the timing box was modified to accept this signal. Thus the start-of-run was exactly synchronized to all other systems. The end-of-run signal was a manual control which was initiated when the vortices were no longer visible because of vortex breakup, smoke disruption, etc. The output of the timing circuit was a momentary relay closure which caused the motorized drive on the 35mm. camera to activate the shutter and advance the film one frame.

Several problems were encountered with this 35mm system:

- a) In the early part of the tests, the timing circuit did not function reliably (e.g., it would not respond to the start-of-run signal, the timing often was not accurate, etc.). These problems were eventually isolated and remedied for the last series of tests.
- b) In a few isolated instances, the motor drive did not function properly for reasons which are not clearly understood.
- c) Installing and removing the 250 exposure cassettes is a fairly complicated and time-consuming task.

In addition to the 35mm system, 16mm or Super 8 movies were taken for most of the tests. The movie camera was mounted on the same tripod as the 35mm camera using a custom-built adaptor, and therefore both systems took essentially the same pictures. The main purpose for the movies was to provide information on vortex behavior in the time interval between 35mm pictures. A secondary, but important use for the movies was as a backup for the 35mm system. When the 35mm system failed, enough data often could be obtained from the movies to provide a limited vortex track for that run. All the movie cameras used suffered from a limited film capacity of three minutes per roll. In some situations it was necessary to reload the camera after every run. With the aircraft turn-around time of 3-5 minutes, the reloading was not an easy task.

2.6 NAFEC PARTICIPATION

NAFEC made all the arrangements to schedule the required aircraft for the tests. The aircraft not available at NAFEC were supplied by the FAA facility in Oklahoma City (B-727), commercial airlines (Pan American World Airways, B-747 and B-707; United Air Lines, B-727), and the USAF (C-5A and C-141). The NAFEC instrumented tower personnel provided expert liaison between TSC staff and the flight crews. The aircraft flight path during the first series of tests and two days (Sept. 11, 12) of the second series of tests was controlled by NAFEC since the calibration of the TSC sensors was not the main purpose of these tests. Hence, for these

tests the flight path generally was not perpendicular to our sensor baseline.

NAFEC supplied the following support during the tests:

a) Tower smoke visualization. Sixteen smoke grenades were placed at each 20 foot interval on a 140' tower. One grenade at each level was ignited for each aircraft pass. Nominally twelve data runs were obtained before the grenades had to be replaced. Four grenades at each level were held in reserve in case of a misfire.

b) Temperature and ambient wind velocity profiles were obtained from sensors at the 23, 45, 70, 100 and 140 foot levels. These data were recorded for a nominal 2-minute span with the mean and standard deviation calculated and reported.

c) Meteorological profiles up to 4000' were obtained from rawinsondes carried by balloons.

d) Phototheodolites tracked the aircraft to provide a very accurate initial position at time $t=0$ for each run. These data were not available for all our tests since it was operational only when NAFEC personnel were taking data using all tower systems (i.e., hot wire anemometers, photographic, etc.). The initial aircraft position was obtained from photographs for the remaining runs (discussed in Section 2.5).

e) The pilot data sheet recorded the salient aircraft parameters for each run: e.g., altitude, airspeed, track, gross weight, flap setting, etc.

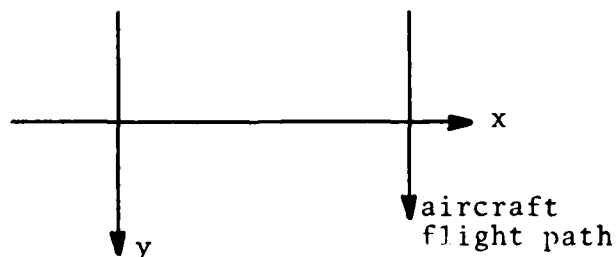
f) Summary test data sheets recorded operational parameters: e.g., temperature, relative humidity, ambient pressure, etc.

3. TEST RESULTS

The salient features of the complete series of tests are given in Table 4. An example of typical data from the propeller anemometer GWVSS is shown in Figures 13 and 14. Although eight channels of data can be displayed in real time on the strip chart recorder, only five data channels can be obtained simultaneously from the tape recorder in a playback mode. A comparison of data from co-located propeller anemometers and pressure sensors is shown in Figures 15 and 16 and includes the runs from Figure 14.

An alternate form of data display is shown in Figure 17. The data from all 12 evenly spaced propeller anemometers appears as z-axis modulations of a CRT, for the same runs of Figure 14. This type of display is possible because of the way the time-shared data is stored by the Ampex SP-700 recorder. Figure 18 shows all 30 time-shared channels for one data run. The channel allocation among the various sensors is typical. Usually at least 12 propeller anemometers and 3 aircraft detectors were operated.

The data taken from an array of five aircraft detectors during the B-747 tests are shown in Figure 19. The co-ordinate system is defined in the following sketch below:



DATA ANALYSIS

The AVCO Corporation produced vortex tracks from the acoustic system magnetic tape using computer programs which were developed on their own initiative and funds in July 1971. The procedure that was used is as follows:

TABLE 4. LIST OF NAFEC TESTS

DATA	AIRCRAFT	RUN NOS.	TYPE OF TESTS	SYSTEMS OPERATING*
4/19/72	DC-7	1-48	Smoke tower fly-bys	1,2
4/20/72	DC-7	49-72	Smoke tower fly-bys	1,2
4/29/72	C-5A	1-13	Smoke tower fly-bys	1,2
5/1/72	880	1-37	Smoke tower fly-bys	1,2
5/2/72	C-141	1-24	Smoke tower fly-bys	1,2
5/5/72	C-880	38-48	Smoke tower fly-bys	1,2
8/17/72	DC-6	1-15	High Altitude	3
8/17/72	DC-6	16-27	Low altitude, no smoke	3,4
8/17/72	DC-6	28-39	Low altitude, no smoke	3,4,5
8/18/72	DC-6	40-51	High altitude	3,4
8/19/72	DC-6	52-87	Smoke tower fly-bys	2,3,4,5
8/22/72	B-727 (UAL)	1-48	Smoke tower fly-bys	2,3,4,5
8/22/72	B-727 (UAL)	1-7	High altitude	3,4
9/11/72	B-727 (FAA)	49-84	Smoke tower fly-bys	2,3,4,5
9/12/72	B-727 (FAA)	85-123	Smoke tower fly-bys	1,2,3,4,5
9/13/72	B-727 (FAA)	8-13	High altitude	3,4
9/13/72	B-727 (FAA)	124-126	Smoke tower fly-bys	1-5
9/14/72	B-727 (FAA)	127-164	Smoke tower fly-bys	1-5
9/14/72	B-727 (FAA)	14-21	High altitude	3,4
9/15/72	B-727 (FAA)	165-200	Smoke tower fly-bys	1-5
9/15/72	B-727 (FAA)	22-23	High altitude	3,4
9/16/72	B-747 (PAA)	1-25	Tower fly-bys	1-5
9/16/72	B-747 (PAA)	1-9	High altitude	3,4
9/17/72	B-747 (PAA)	10-21	High altitude	3,4
9/17/72	B-747 (PAA)	26-52	Smoke tower fly-bys	1-5
10/16/72	C-880	49-72	Smoke tower fly-bys	2-5
10/16/72	C-880	1-12	High altitude	3,4
10/17/72	B-747 (PAA)	53-76	Smoke tower fly-bys	2-5
10/17/72	B0747 (PAA)	22-30	High altitude	3,4
10/18/72	B-707 (PAA)	1-33	Smoke tower fly-bys	2-5

*See page 28.

TABLE 4. LIST OF NAFEC TESTS (CONTINUED)

DATA	AIRCRAFT	RUN NOS.	TYPE OF TESTS	SYSTEMS OPERATING*
10/18/72	B-707 (PAA)	1-17	High altitude	3,4
10/18/72	C-880	13-29	High altitude	3,4
10/20/72	C-880	30-68	High altitude	3,4,5
11/1/72	B-707 (PAA)	34-63	Smoke tower fly-bys	2-5
11/1/72	B-707 (PAA)	18-31	High altitude	2-5

- *1 - Pressure Sensors
- 2 - Photographic Tracking
of Tower Smoke
- 3 - Acoustic Tracking
- 4 - Propeller Anemometers
- 5 - Aircraft Detector
Pressure Sensor

Total Number of Tests		
AIRCRAFT	SMOKE TOWER FLY-BYS	HIGH ALTITUDE
DC-6	34	27
DC-7	72	0
C-880	72	68
C-141	24	0
C-5A	13	0
B-727	200	33
B-707	63	31
B-747	76	30

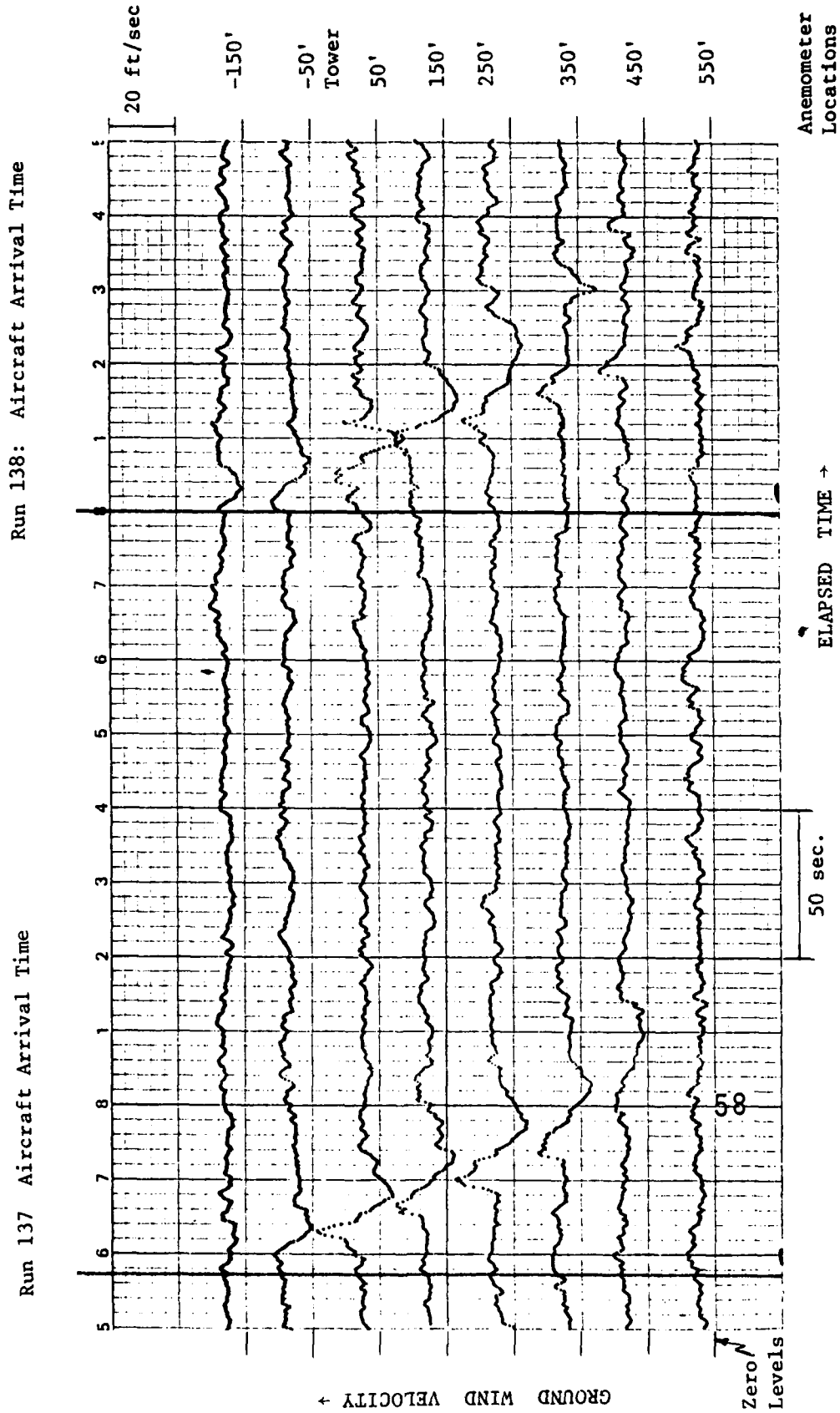


FIGURE 13. PROPELLER ANEMOMETER DATA, 9/14/72, B-727 AIRCRAFT. AIRCRAFT ALTITUDE = 130', AIRCRAFT LATERAL POSITION = -150'

Run 30: Aircraft Arrival Time

Run 31: Aircraft Arrival Time

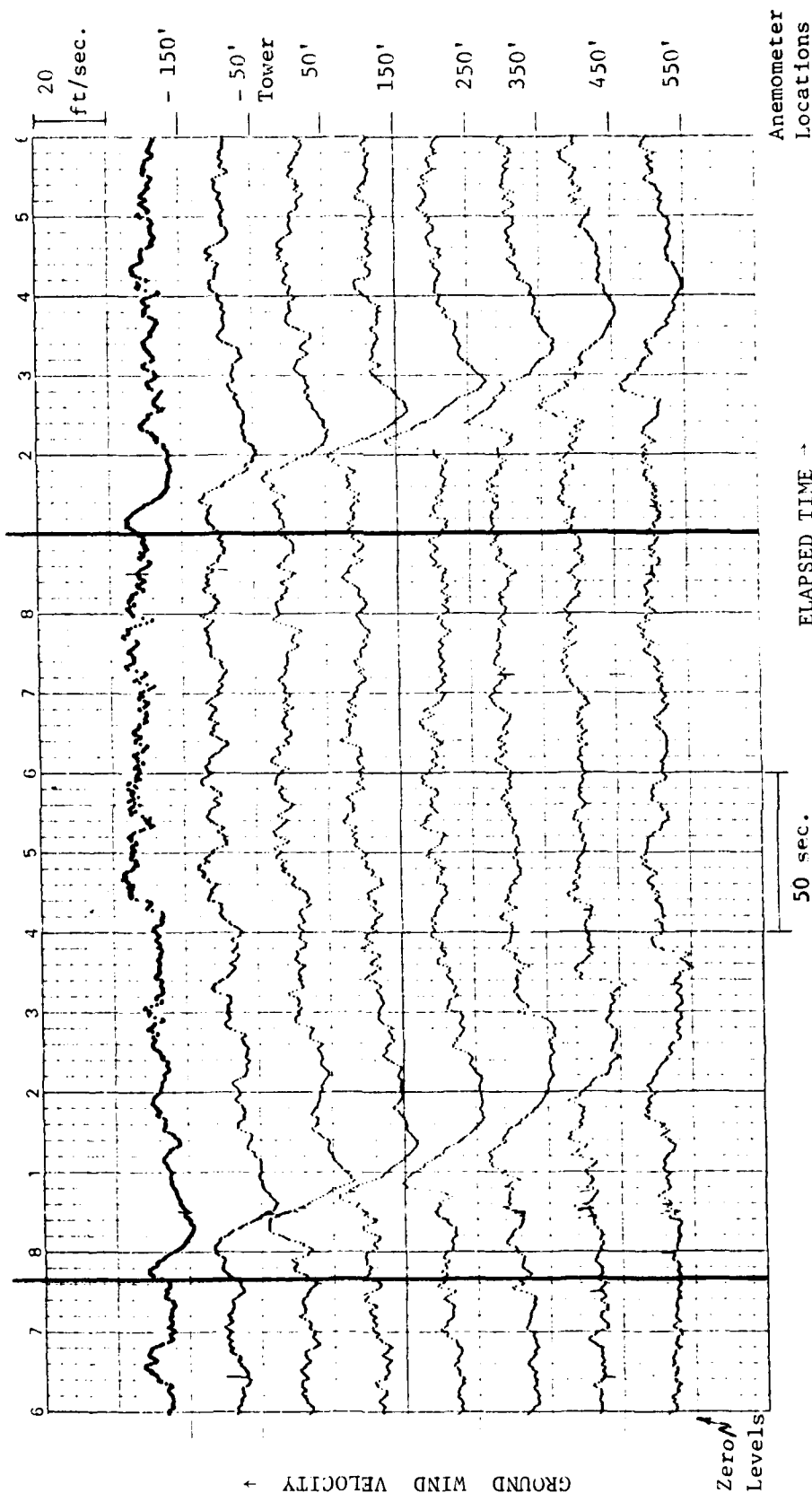


FIGURE 14. PROPELLER ANEMOMETER DATA, 9/17/72, B-747 AIRCRAFT. AIRCRAFT ALTITUDE = 150', AIRCRAFT LATERAL POSITION = -200'

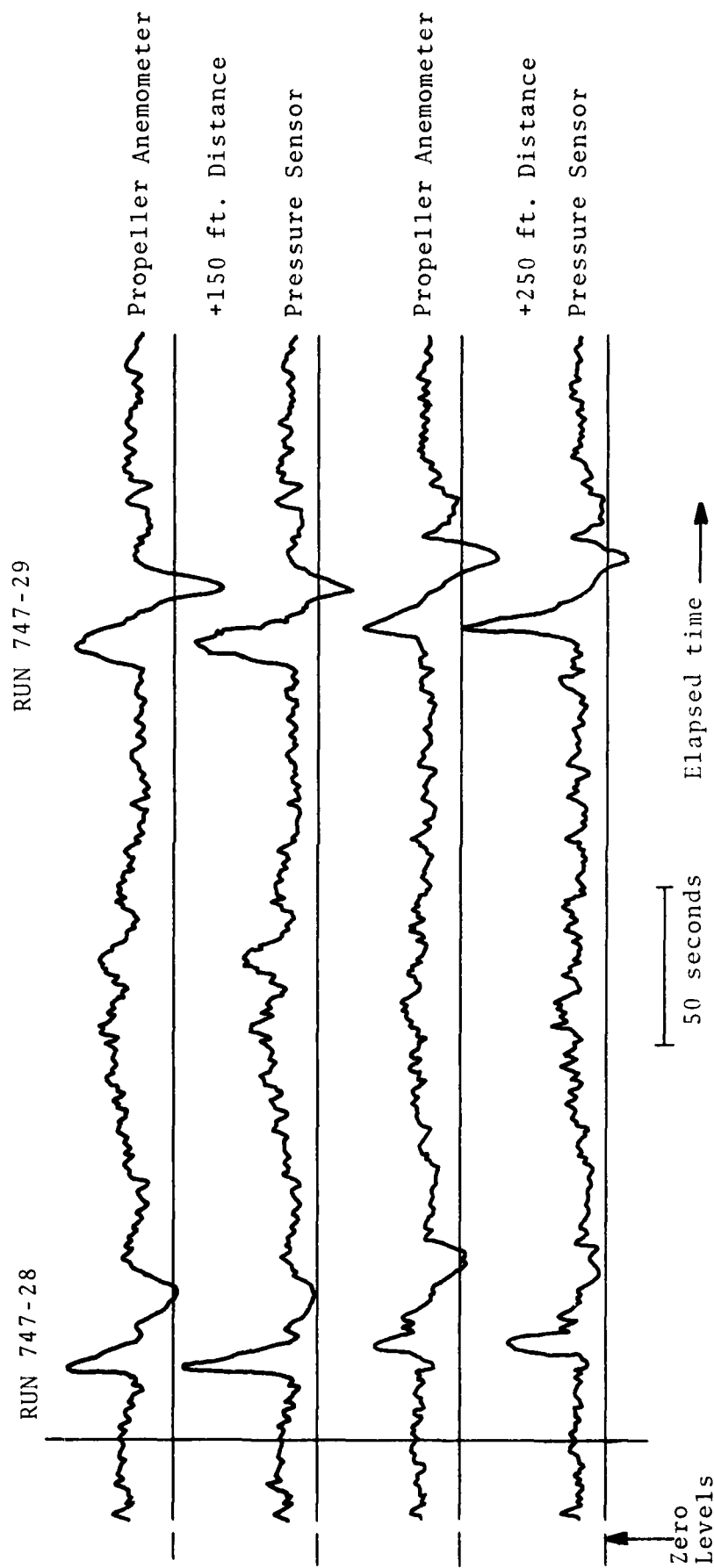


FIGURE 15. COMPARISON OF PRESSURE SENSOR AND PROPELLER ANEMOMETER DATA OF RUNS 747-28, 29

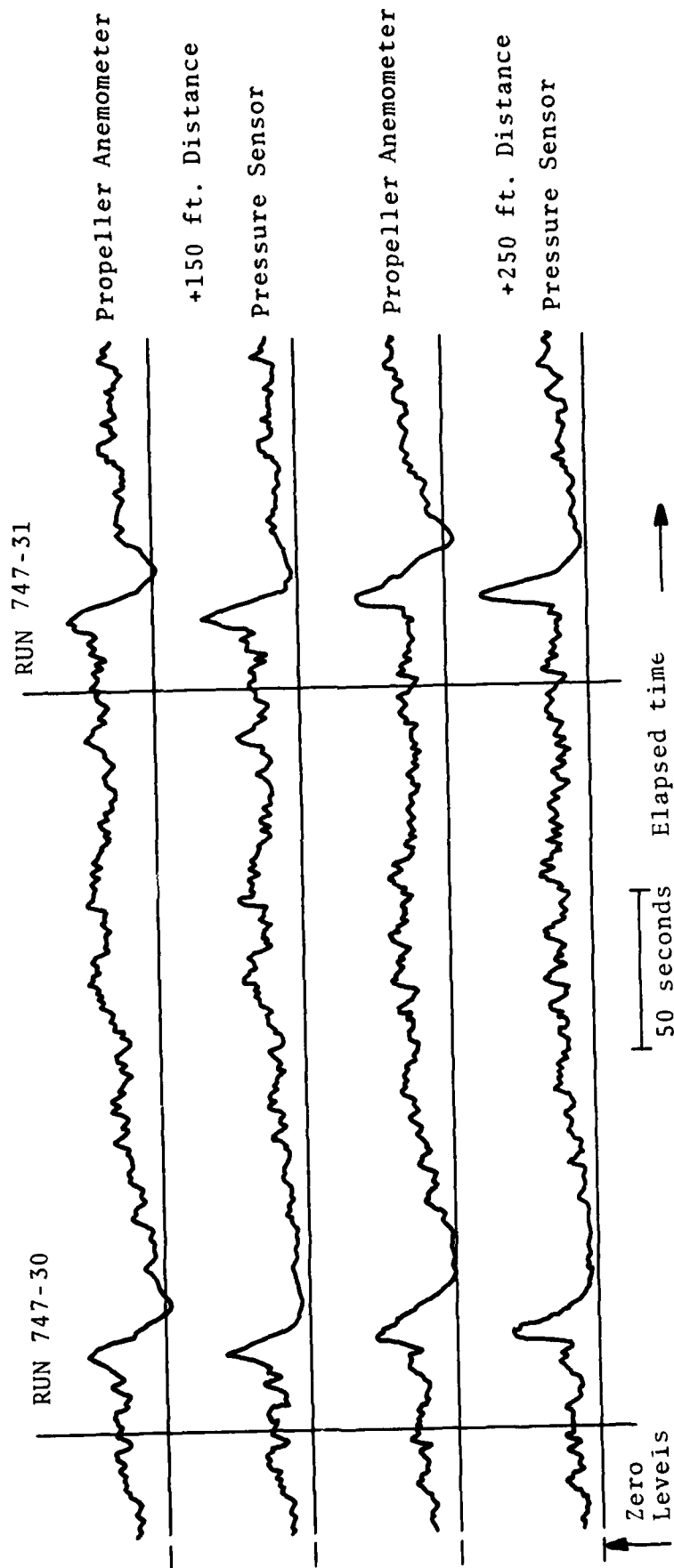


FIGURE 16. COMPARISON OF PRESSURE SENSOR AND PROPELLER ANEMOMETER DATA OF RUNS 747-30, 31

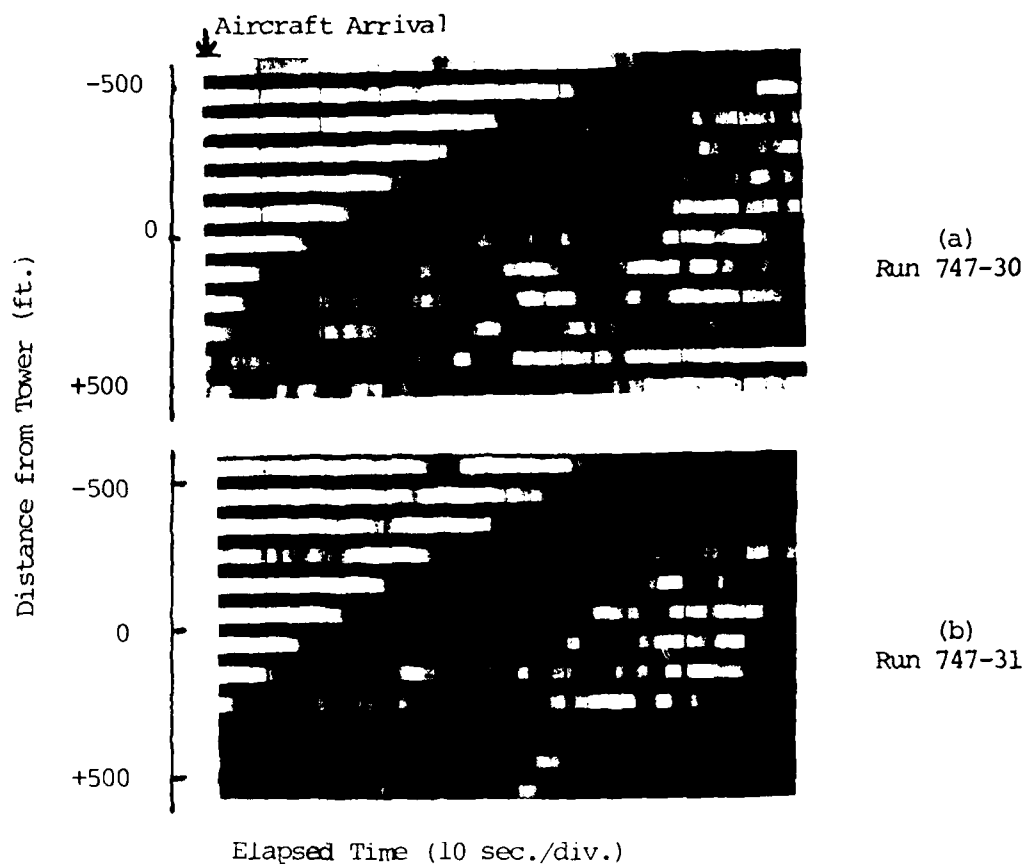


FIGURE 17. VORTEX TRACKS FROM PROPELLER ANEMOMETER DATA

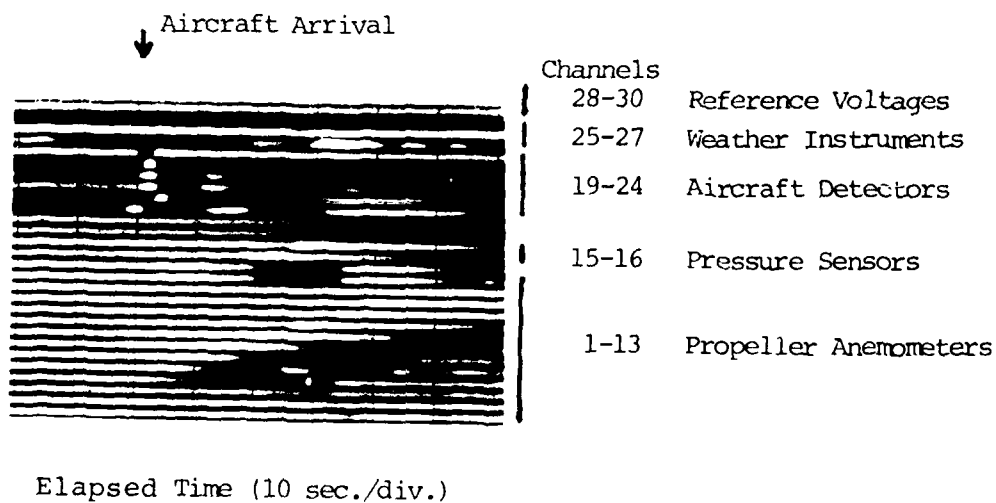


FIGURE 18. TAPE RECORDER CHANNEL USE WITH DATA OF RUN 747-26

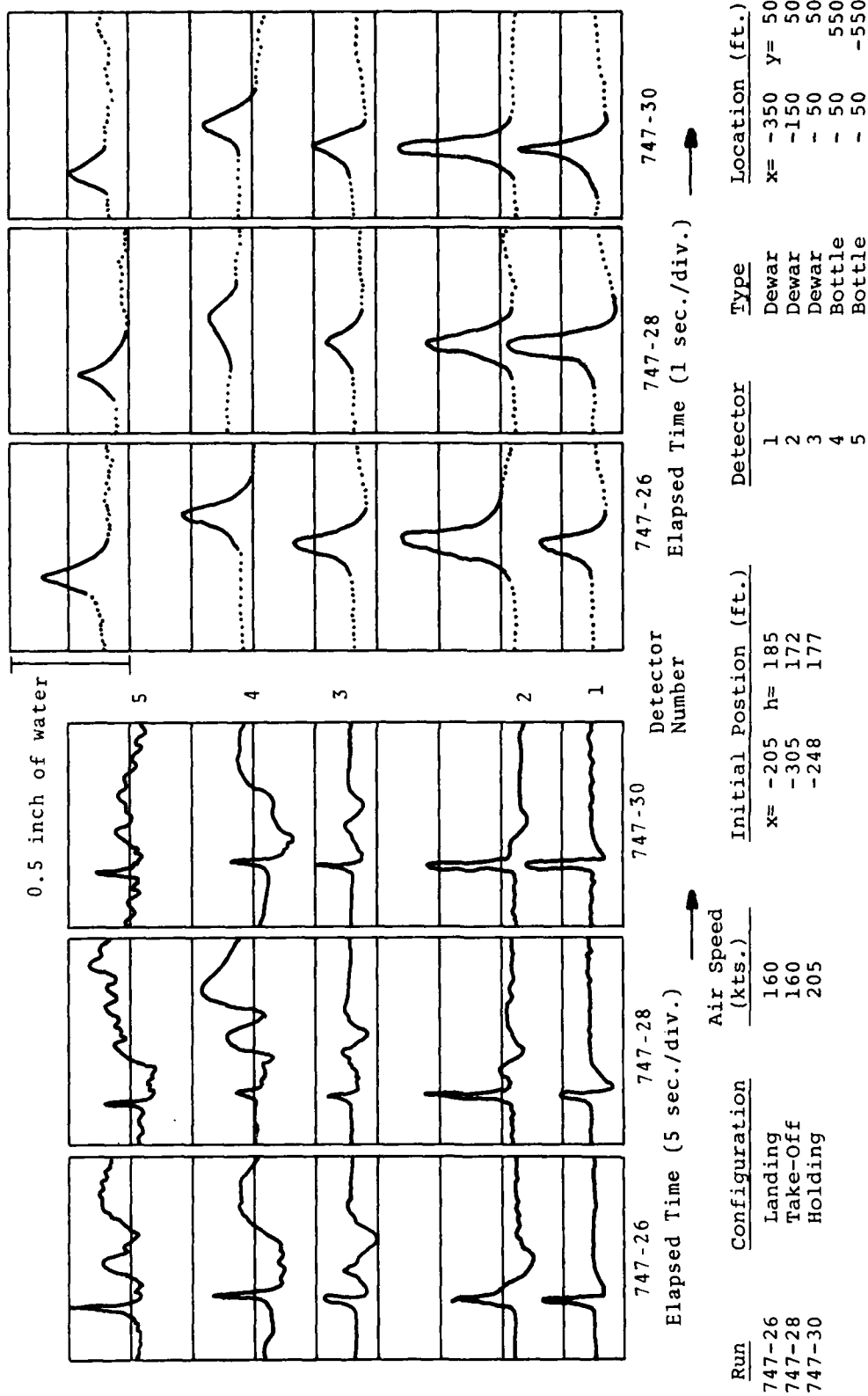


FIGURE 19. AIRCRAFT DETECTOR DATA

- a) The analog data are converted to digital form.
- b) For each receiver, the nine highest peaks for each period are determined. A running integration of approximately 3 msec (one pulse width) is used to suppress unwanted peaks.
- c) The position of the leading edge of the pulse is then determined by subtracting a small time increment from the position of the peak. The amount of time subtracted from the ground pulse signal is different from that subtracted from the vortex return signal; both were empirically determined. The leading edge position is then plotted in the form of an acoustogram with the relative strengths indicated (the lowest number represents the largest signal). Figure 20a shows an example of such an acoustogram. The abscissa is labeled by frame (sweep) number and can be converted to running time by multiplying by the period. The ordinate is labeled by sample number and can be converted to time by dividing by the sampling rate (1600 samples/sec.).
- d) The acoustograms are then visually scanned to determine what areas contain useful data. The remaining regions are eliminated from consideration. The resultant modified acoustogram is shown in Figure 20b.
- e) The computer then measures the time delays from this adjusted acoustogram. The arrival time for each ground signal is kept fixed for the entire data run. The vortex position is calculated using the time delays from all possible combinations of transmitters and receivers. Figure 21 shows a vortex track obtained by this method. The vertical bracket indicates the standard deviation of the calculated positions, weighted according to their sensitivity to timing errors. The number inside the bracket indicates the number of combinations of receivers and transmitters used.
- f) Final plots are then produced by a weighted average of 5 frames of the data in Figure 21. A total of 61 data runs were reduced by this technique. (See Table 4.) Administrative problems prevented the processing of the complete test series.

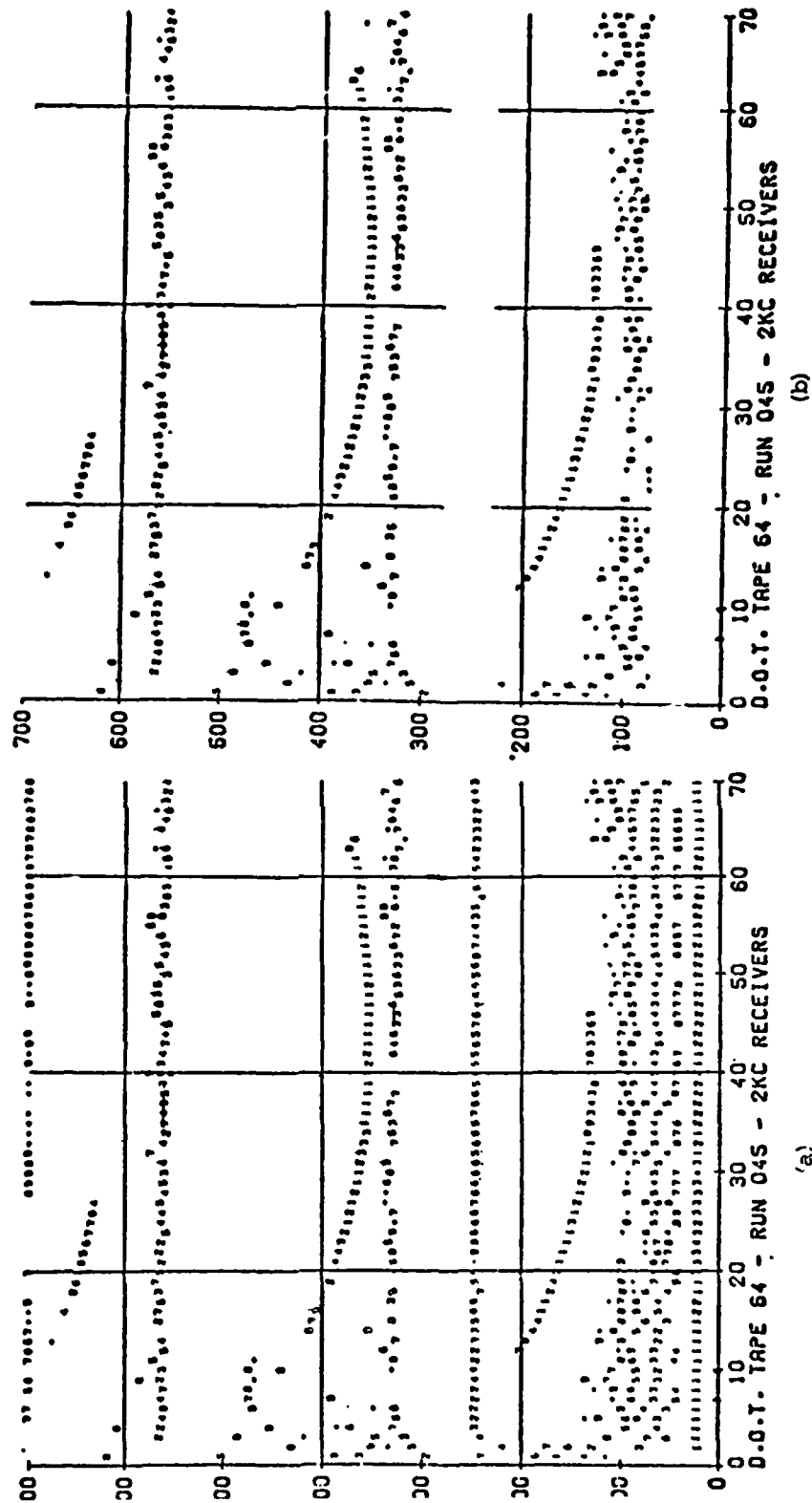


FIGURE 20. COMPUTER PRODUCED ACOUSTOGRAMS

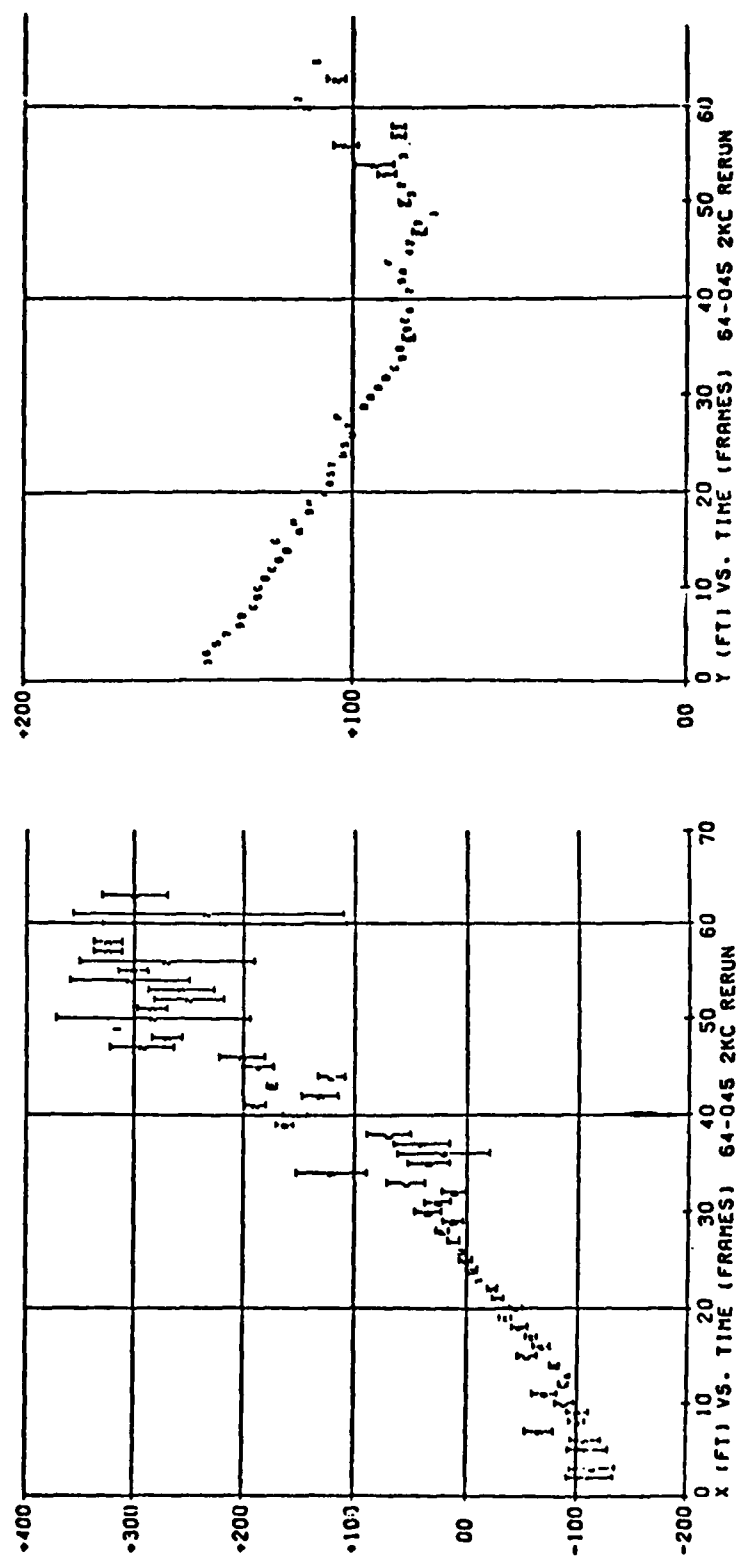


FIGURE 21. COMPUTER PRODUCED VORTEX TRACKS

The data from the ground wind system were manually processed by determining the time of occurrence of the maximum (first vortex) or minimum (second vortex) signal for each anemometer. It is assumed that these peaks in the signals imply that the center of the vortex was directly over the sensor.

The data from the photographic system were processed to obtain the position of the vortex to be used as a standard for calibrating the various sensors. Determining the location of the vortex center is very difficult unless the flight path is parallel to a line between the tower and the camera so that the observer can look approximately down the axis of the vortex. This problem was recognized during the first series of tests, in which the aircraft flight paths were controlled by NAFEC and seldom had this optimal orientation. In the second series of tests, the aircraft flight path was controlled by TSC, was always essentially parallel to the camera-tower line, and pointed toward the camera to make use of aircraft crabbing (as described in Section 2.5).

In order to track a vortex it is necessary to identify some circular feature in the entrained smoke. Two basic forms are observed:

a) A clear "hole" in the central core area, which occurs when the vortex core passes between smoke grenades and for tubular vortices where the axial flow redistributes the smoke in the core region.

b) A fairly dense spot of smoke, which occurs when the core of a vortex passes near a smoke grenade and a large volume of smoke is captured in the core.

Once the center of the vortex is located, a scaling technique and basic trigonometry are used to obtain the actual location. (See Appendix A.) The tower (140' high) is used as a reference scale for the height and the TSC-installed sign posts are used as a reference scale for the horizontal position.

A comparison of the data obtained from the sensors with the position of the vortex as obtained from the photographs is given in Figures 22-34. A summary showing the run numbers and the figure number where the data can be found is given in Table 5.

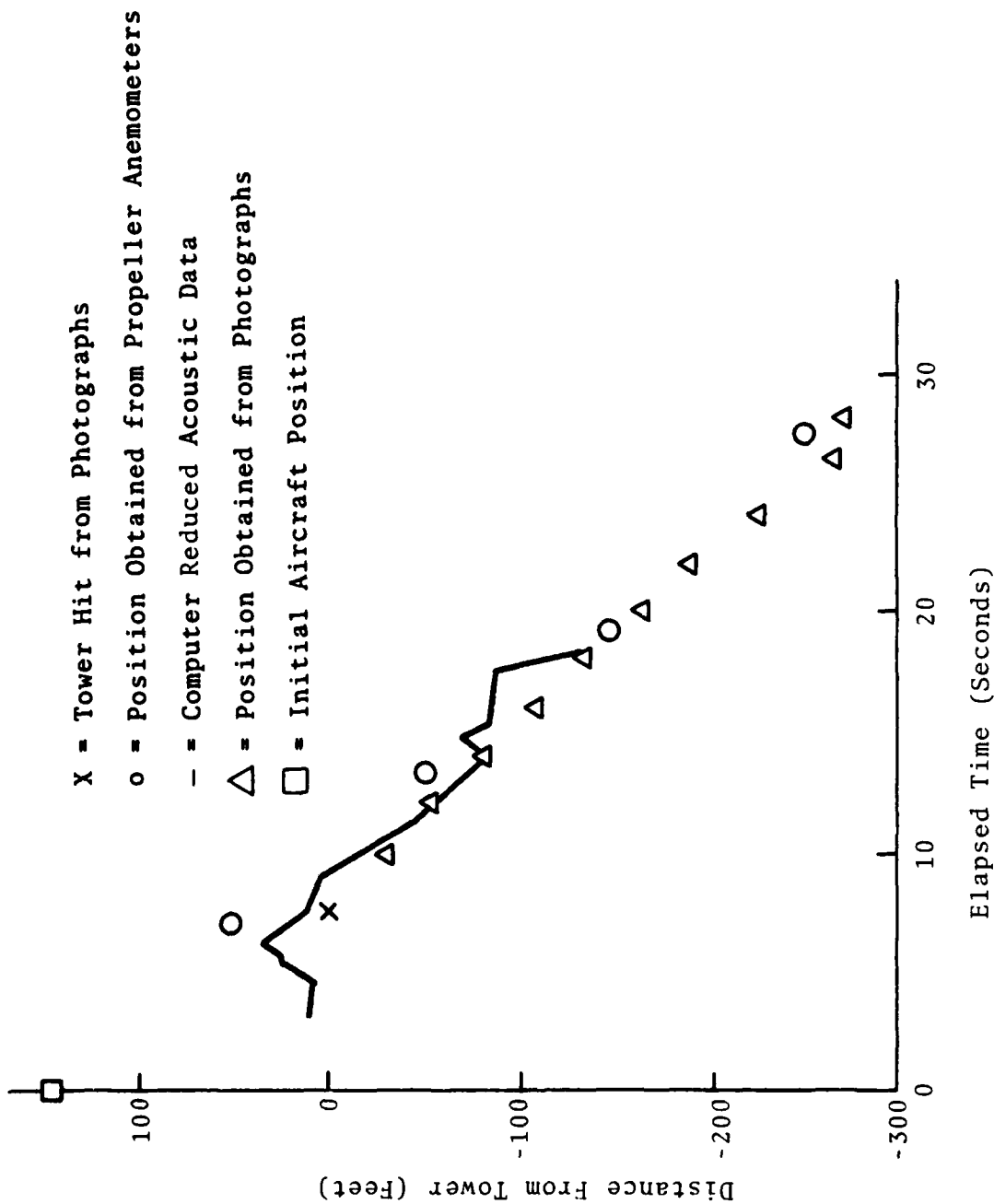


FIGURE 22. NAFEC TOWER TESTS, 9/15/72, RUN 727-178 DOWNWIND VORTEX

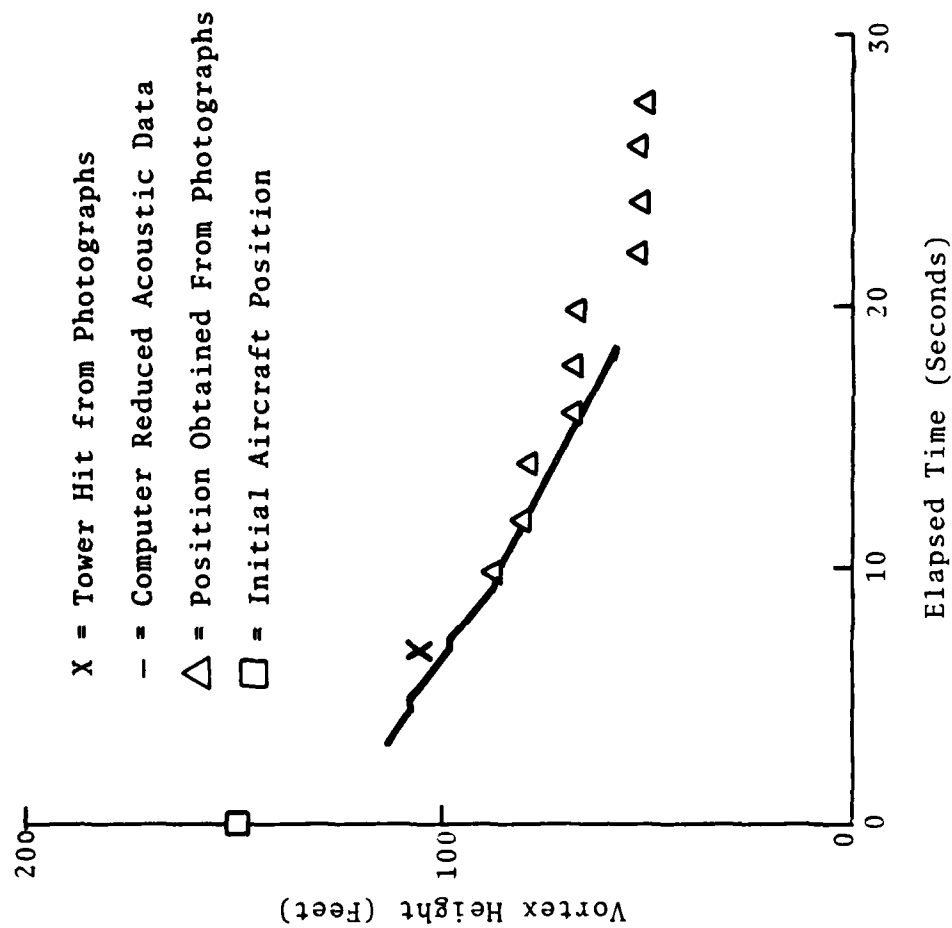


FIGURE 22. (CONCLUDED)

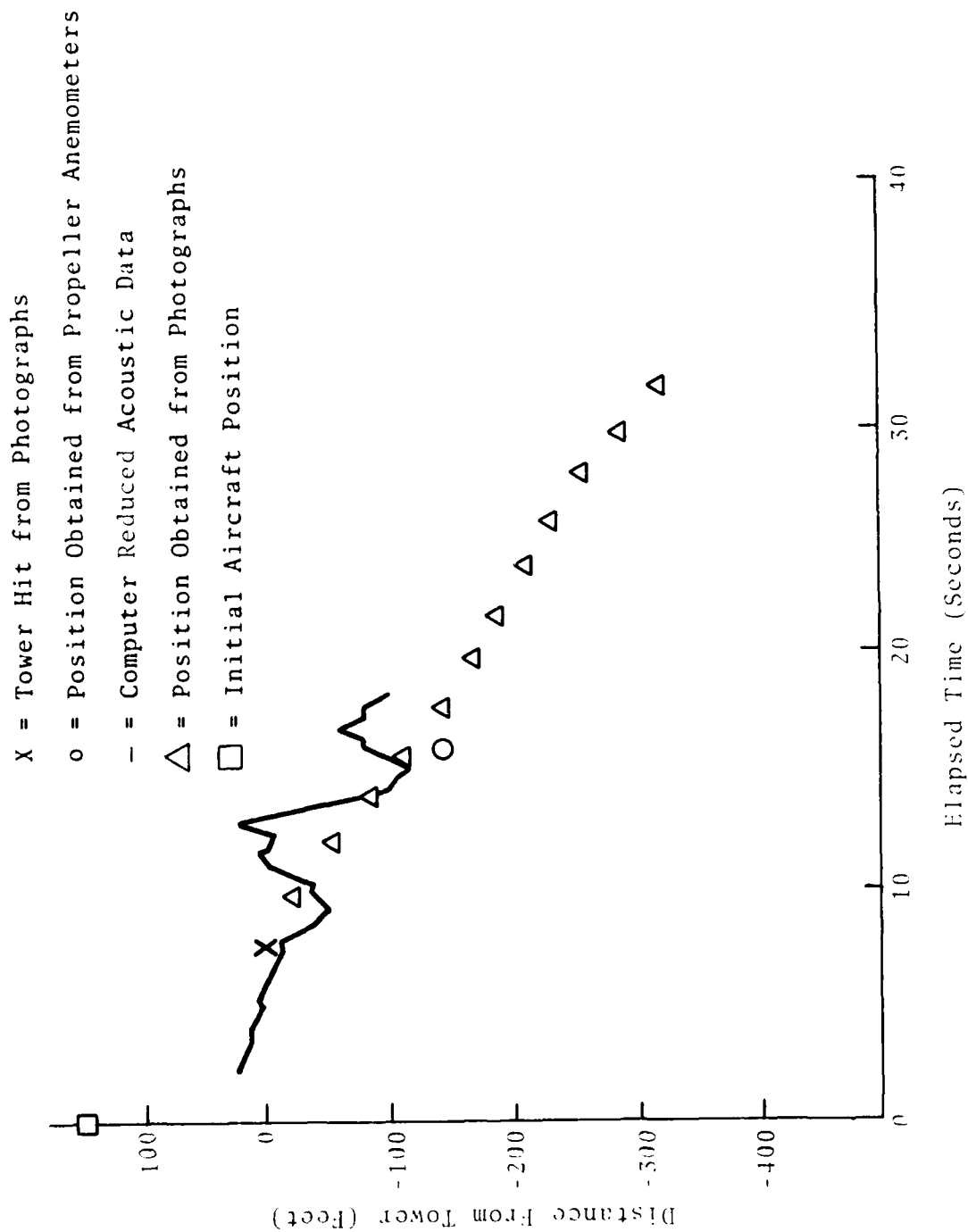


FIGURE 23. NAFEC TOWER TESTS, 9/15/72, RUN 727-180 DOWNWIND VORTEX

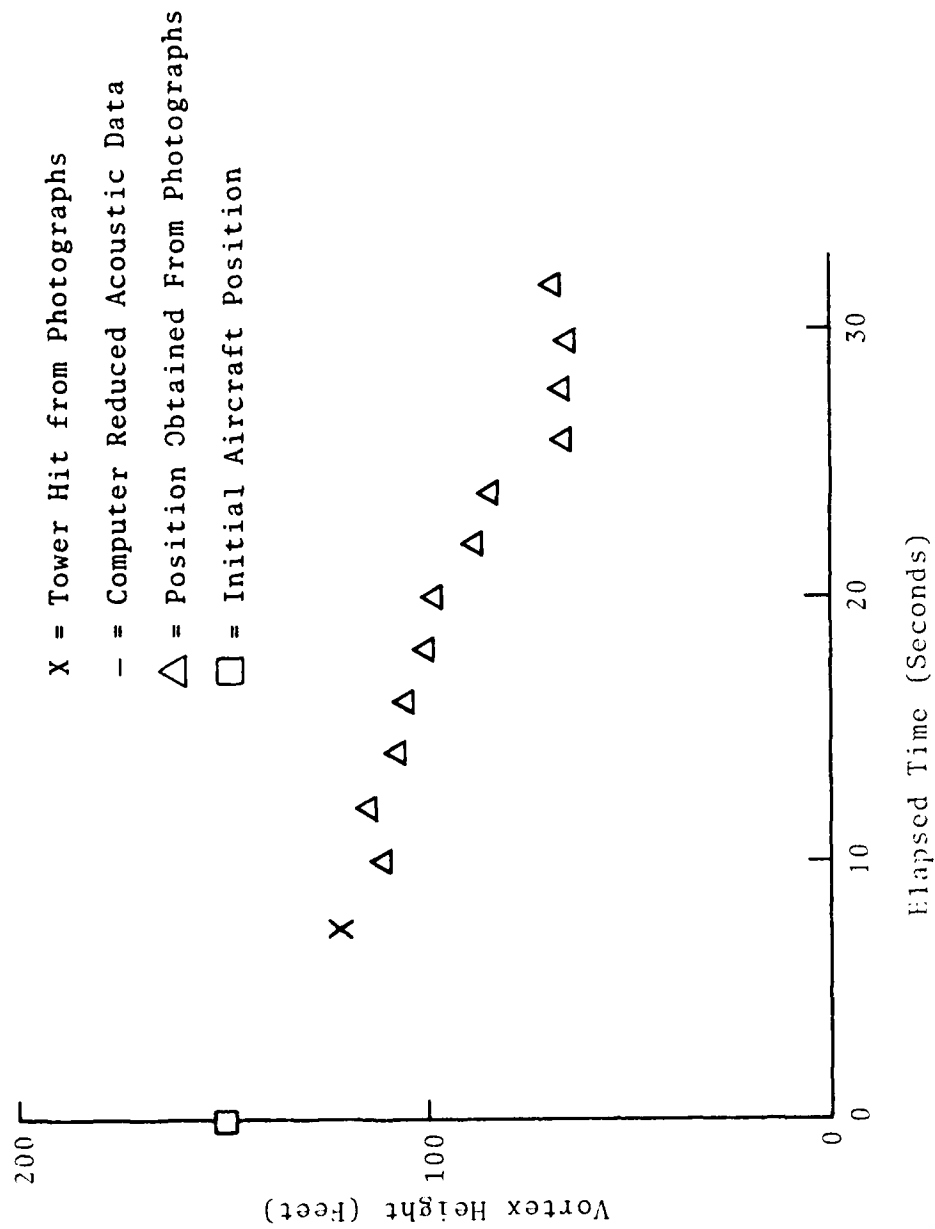


FIGURE 23. (CONCLUDED)

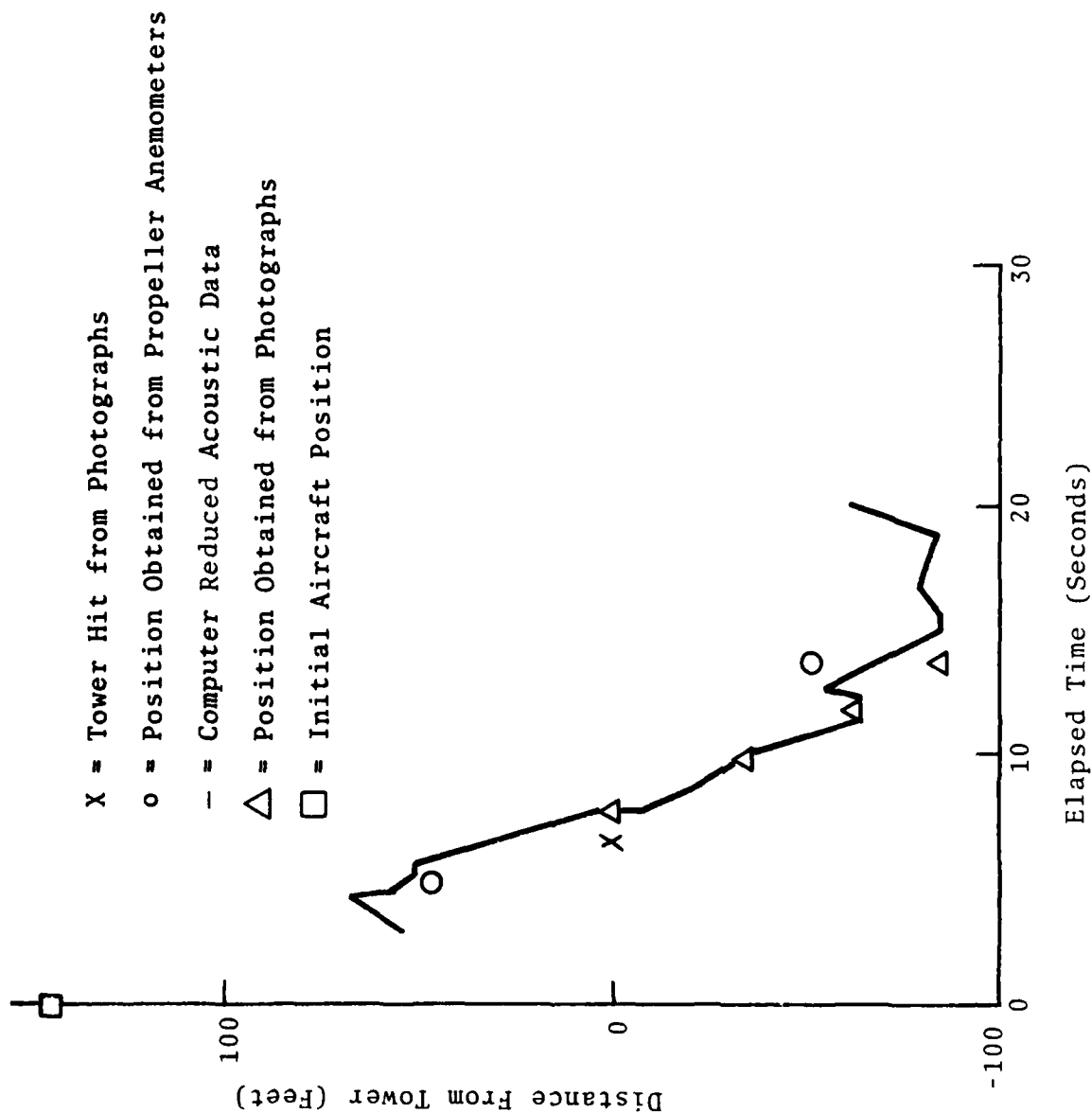


FIGURE 24. NAFEC TOWER TESTS, 9/15/72, RUN 727-181 DOWNWIND VORTEX

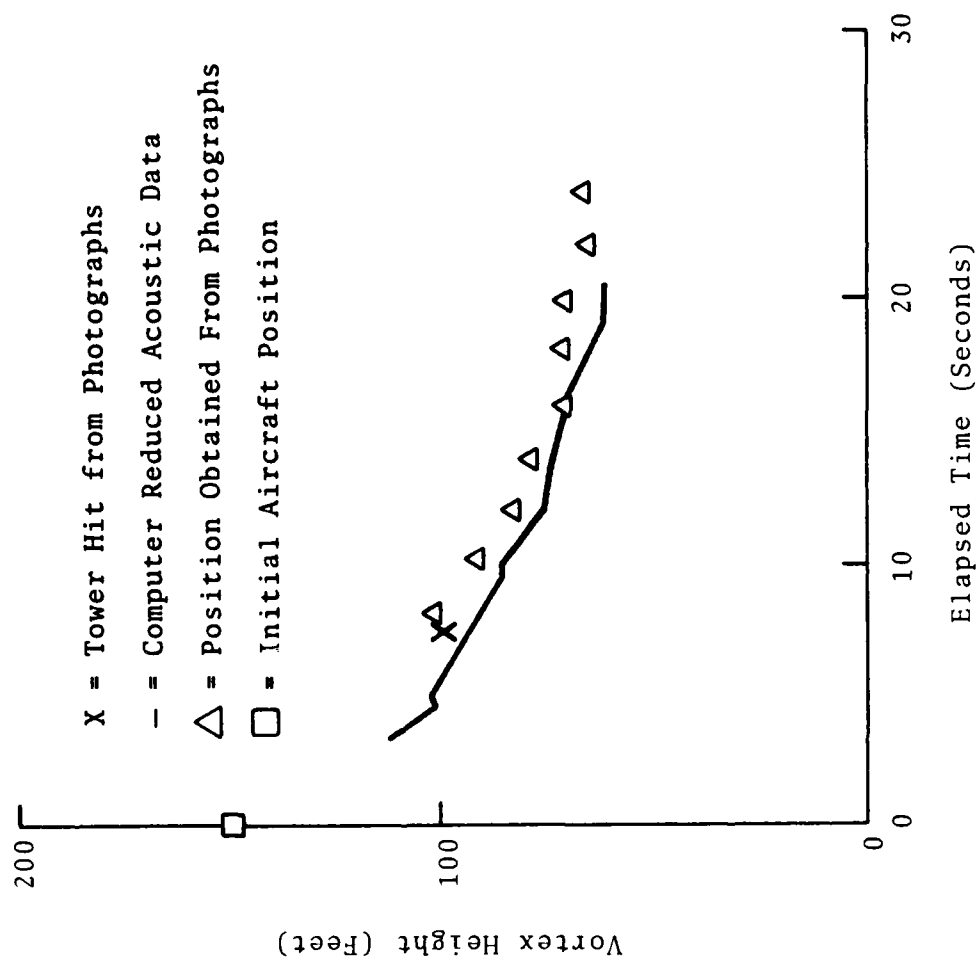


FIGURE 24. (CONCLUDED)

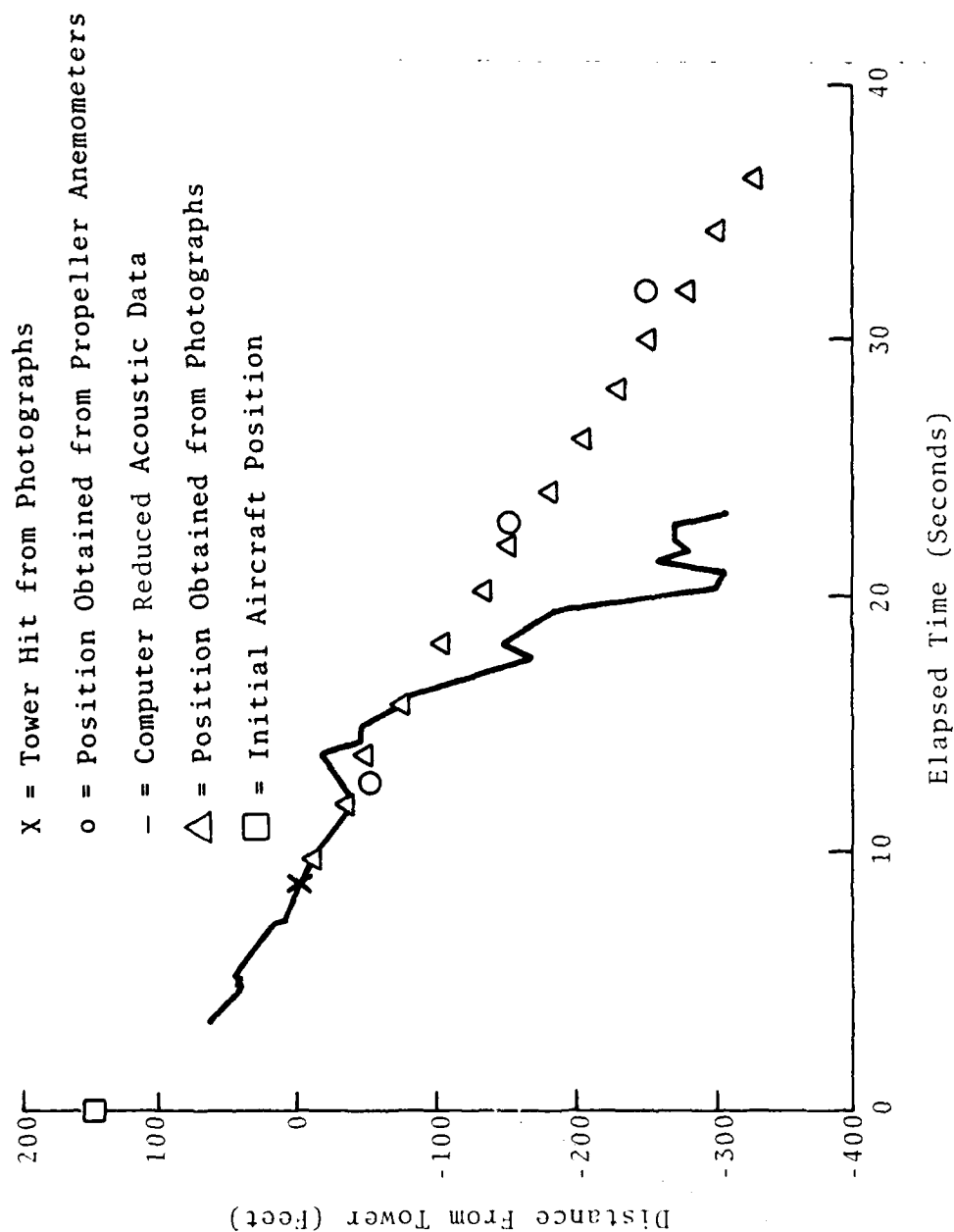


FIGURE 25. NAFEC TOWER TESTS, 9/15/72, RUN 727-182 DOWNWIND VORTEX

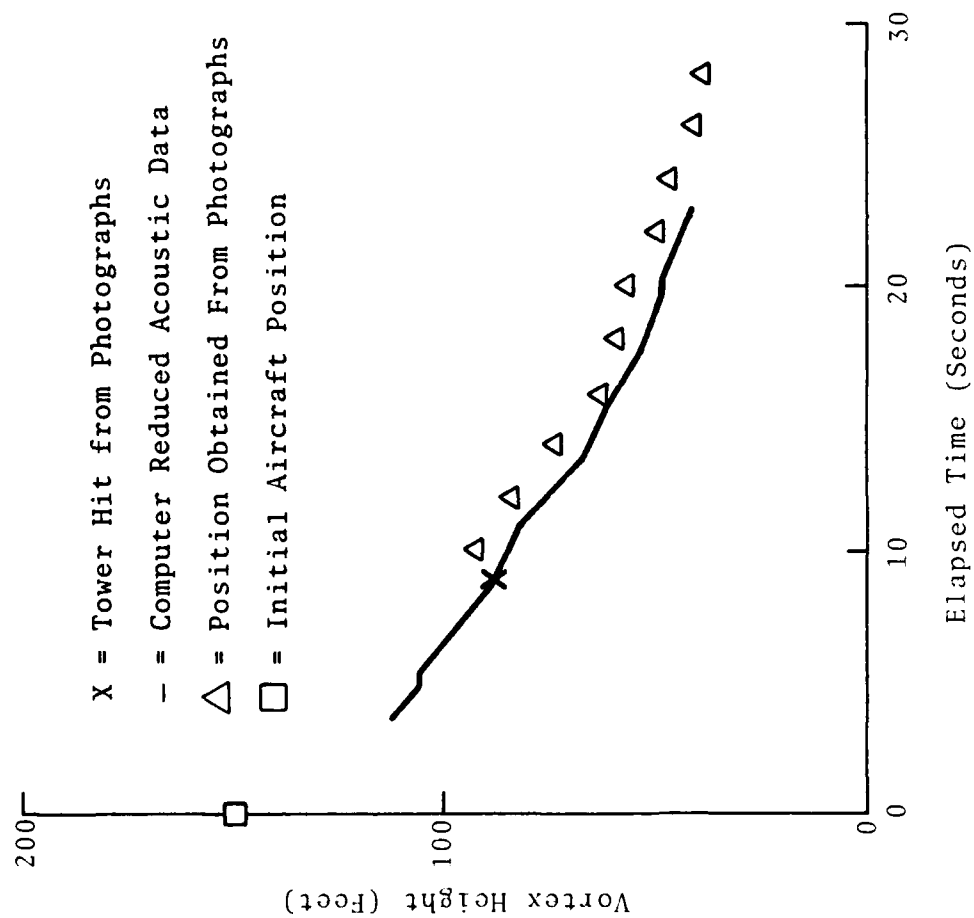


FIGURE 25. (CONCLUDED)

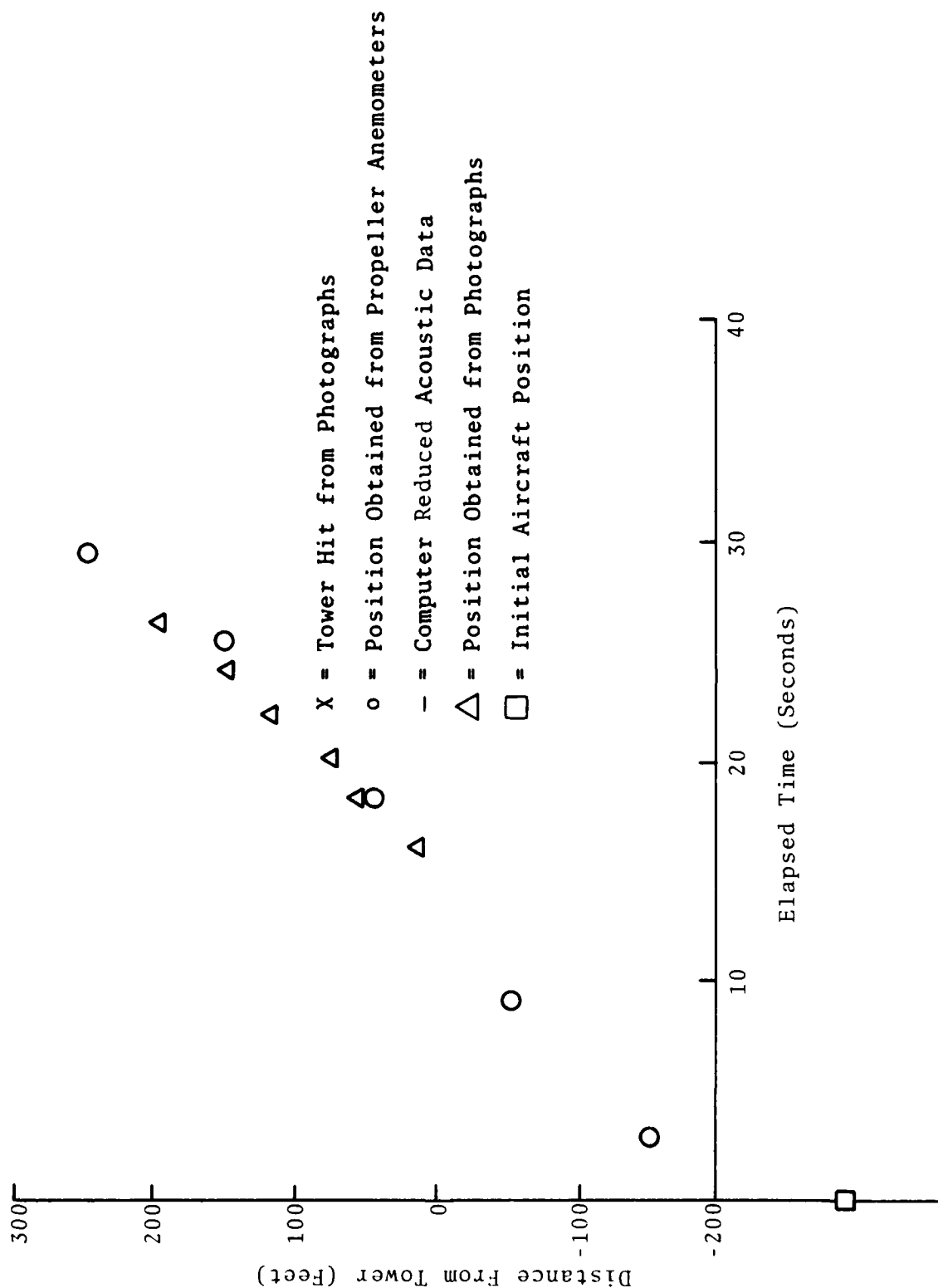


FIGURE 26. NAFEC TOWER TESTS, 9/17/72, RUN 747-42 DOWNWIND VORTEX

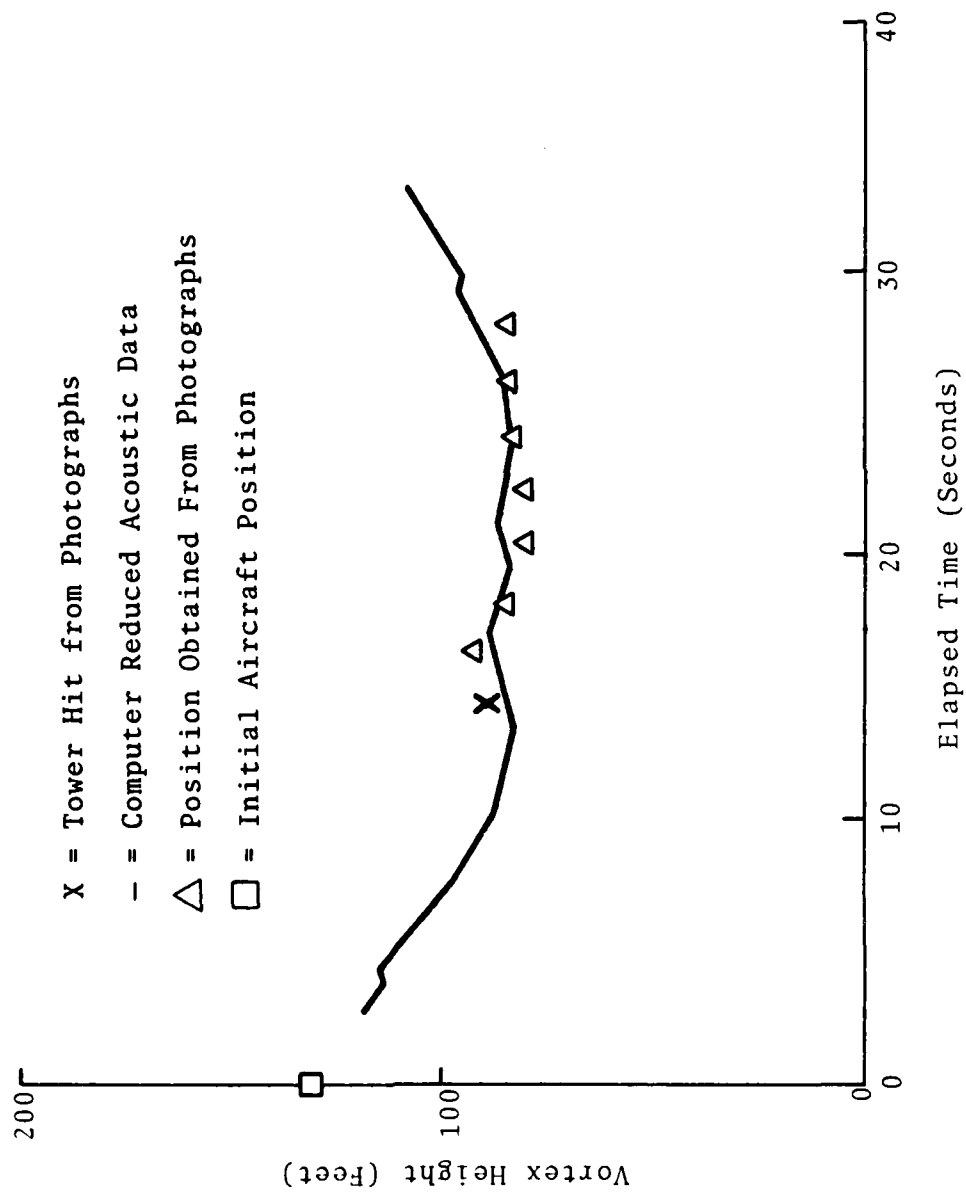


FIGURE 26. (CONCLUDED)

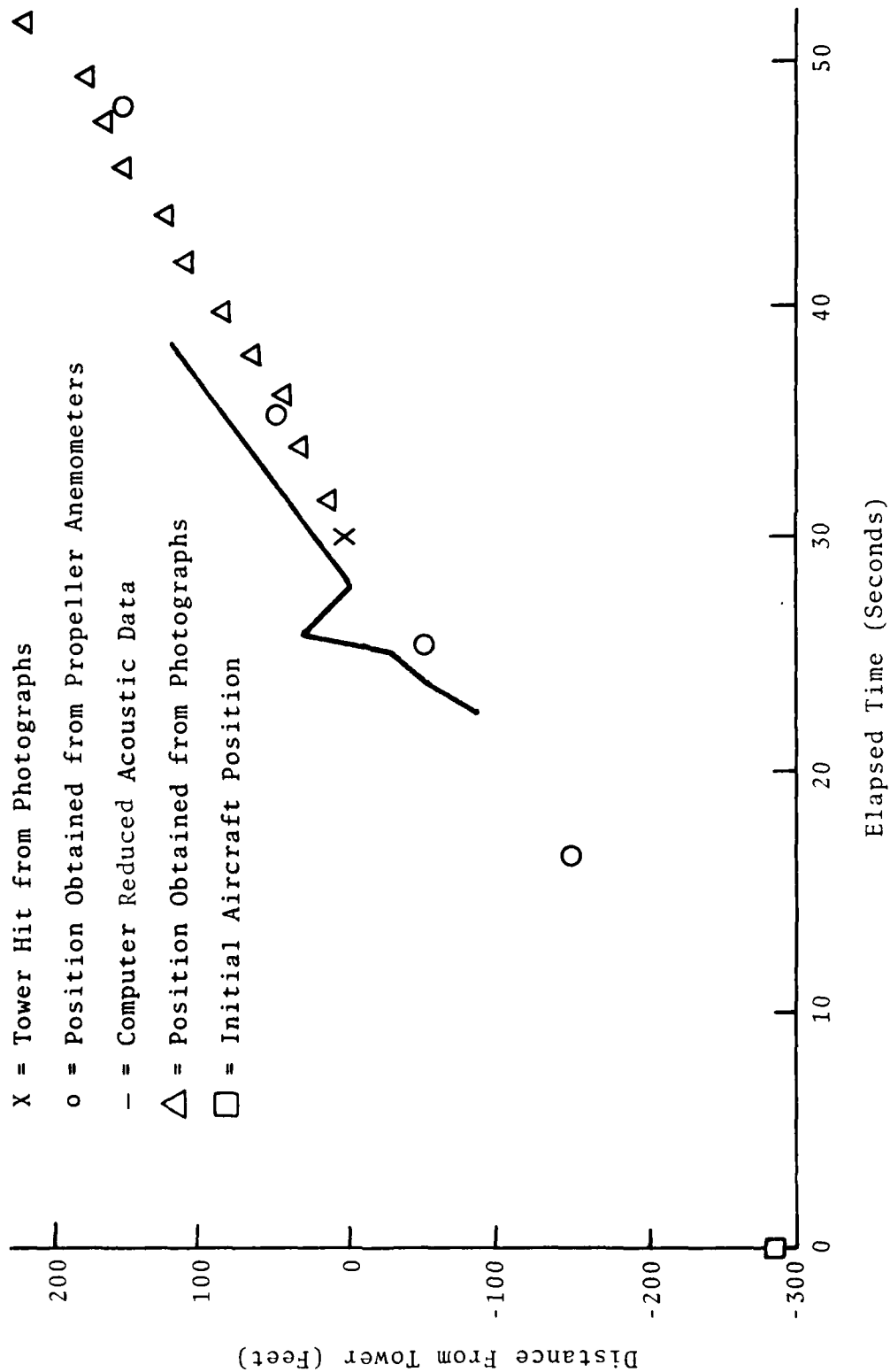
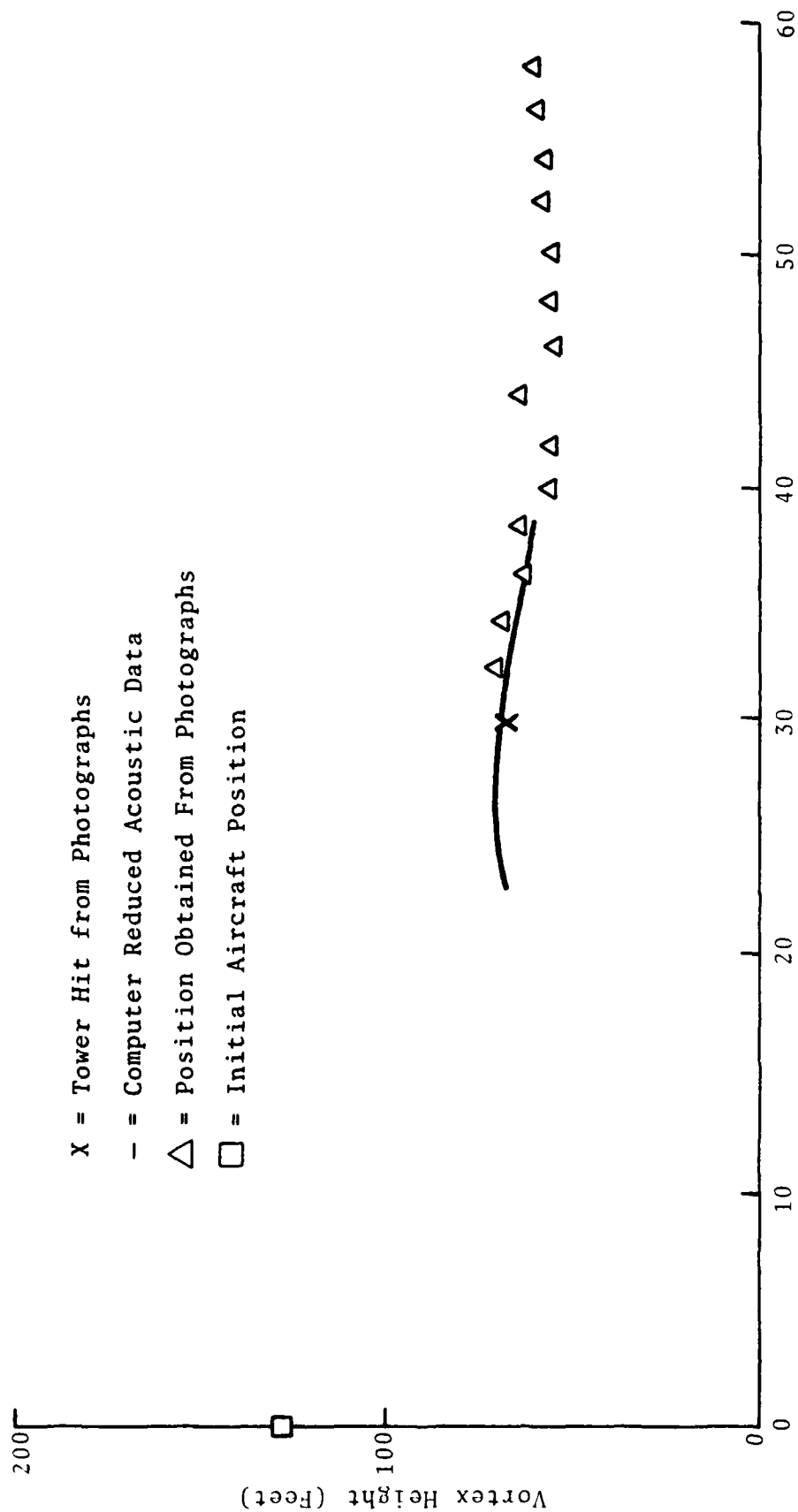


FIGURE 27. NAFEC TOWER TESTS, 9/17/72, RUN 747-42 UPWIND VORTEX



Elapsed Time (Seconds)

FIGURE 27. (CONCLUDED)

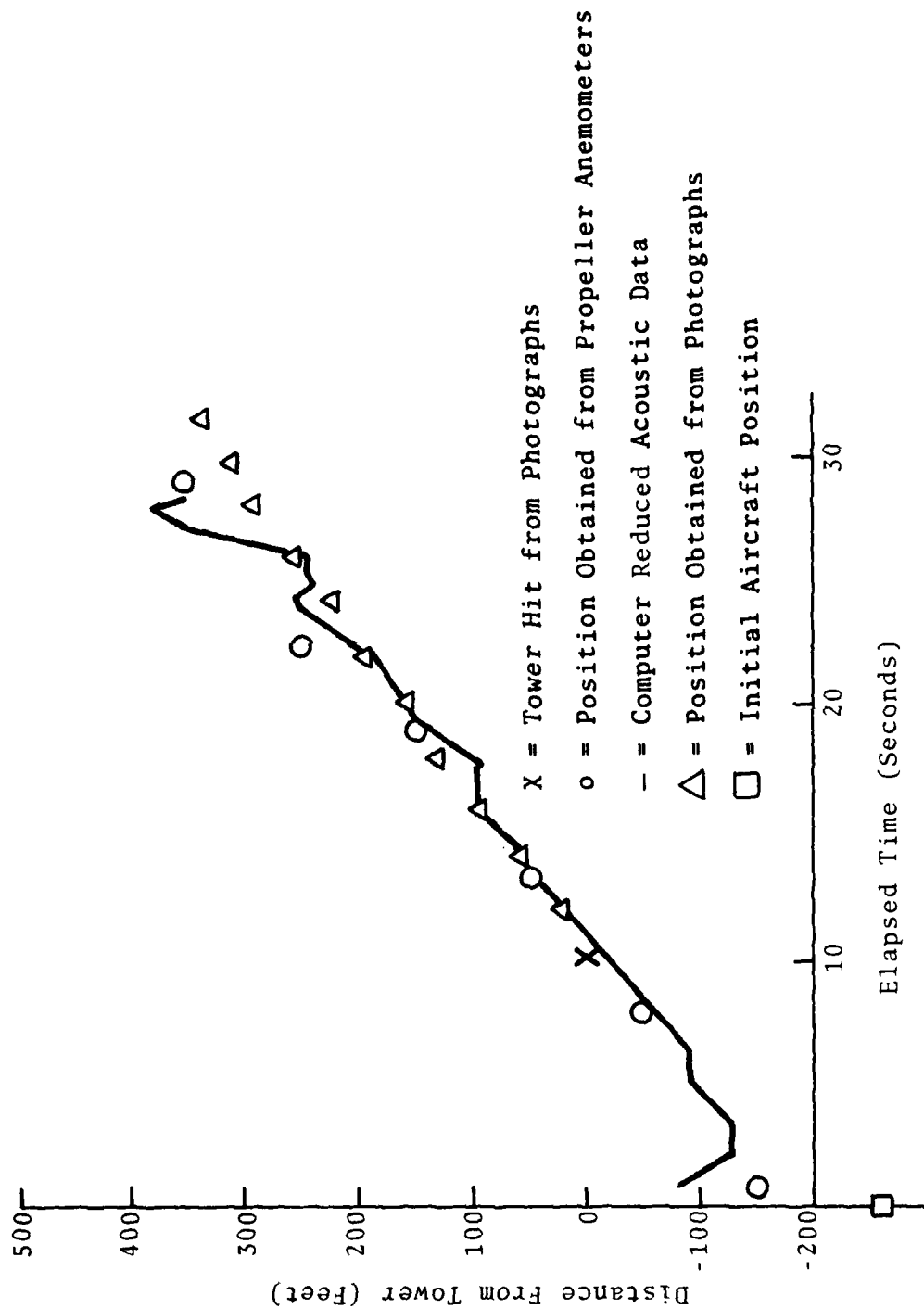


FIGURE 28. NAFEC TOWER TESTS, 9/17/72, RUN 747-43 DOWNWIND VORTEX

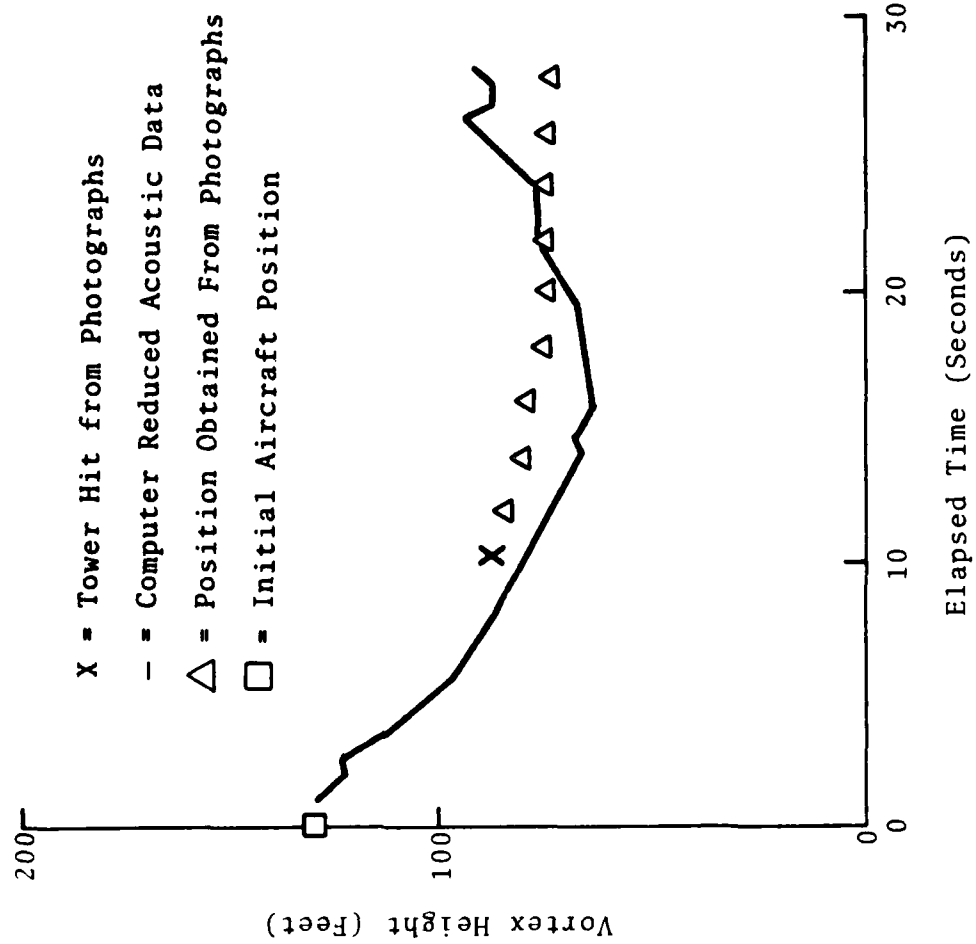


FIGURE 28. (CONCLUDED)

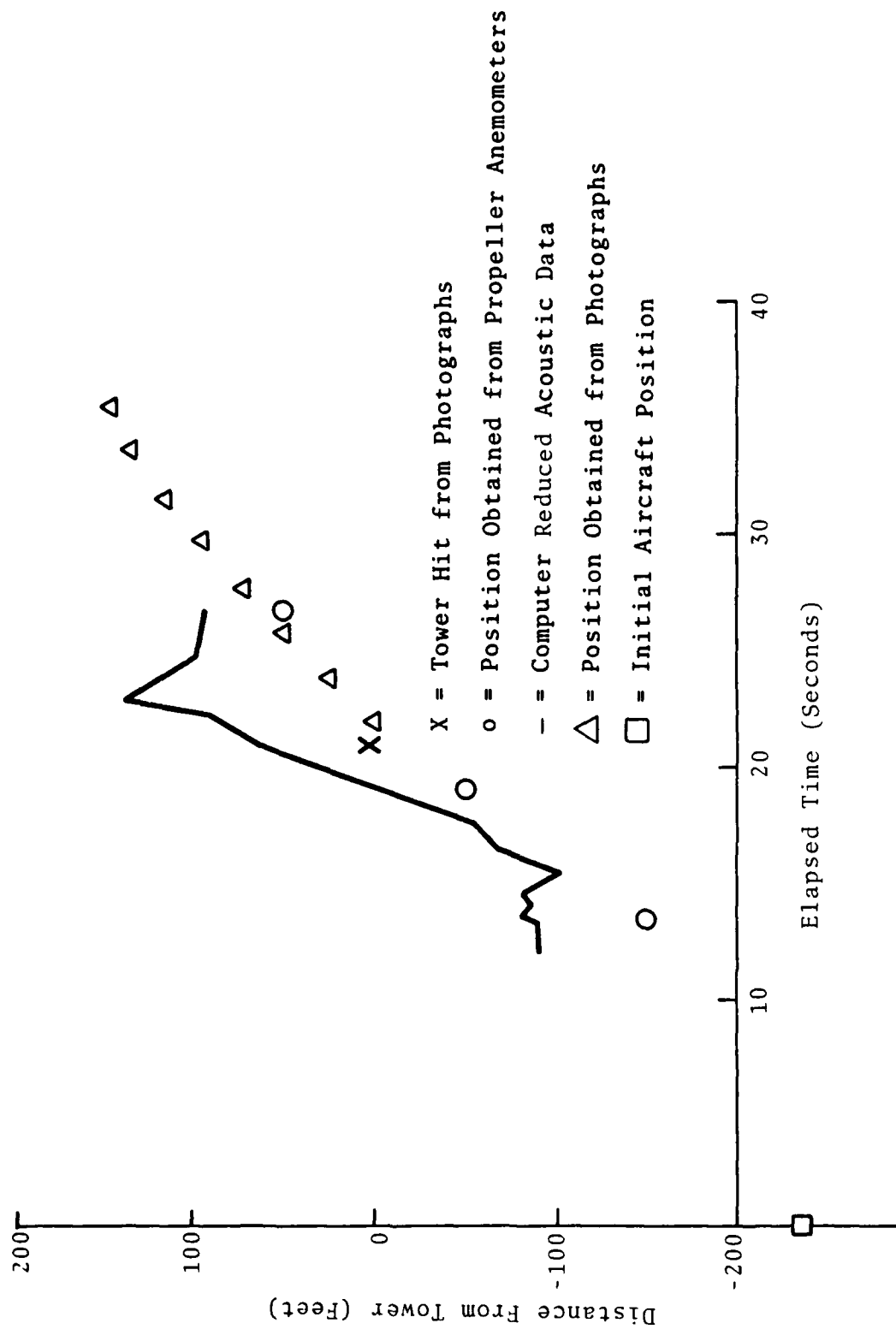


FIGURE 29. NAFEC TOWER TESTS, 9/17/72, RUN 747-43 UPWIND VORTEX

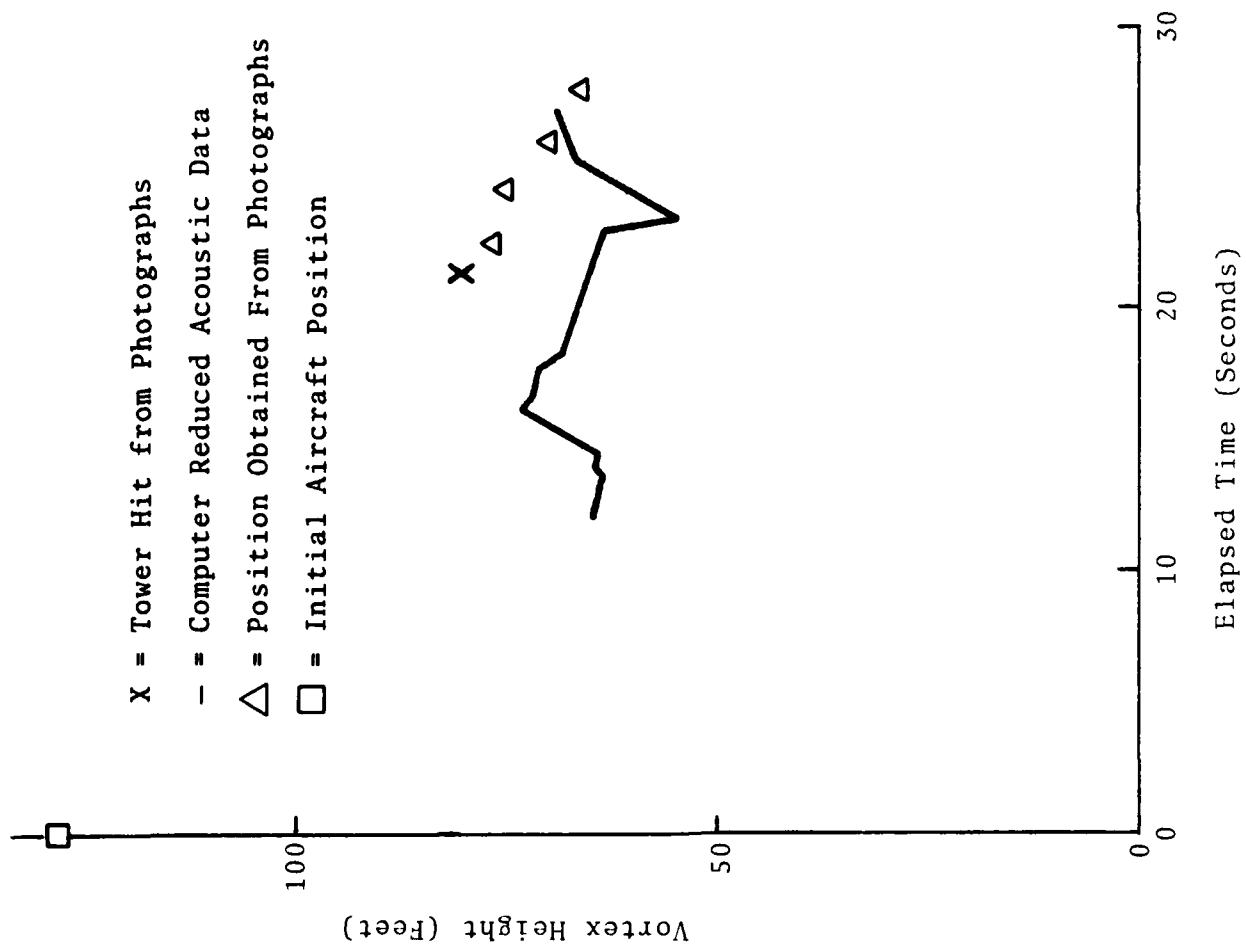


FIGURE 29. (CONCLUDED)

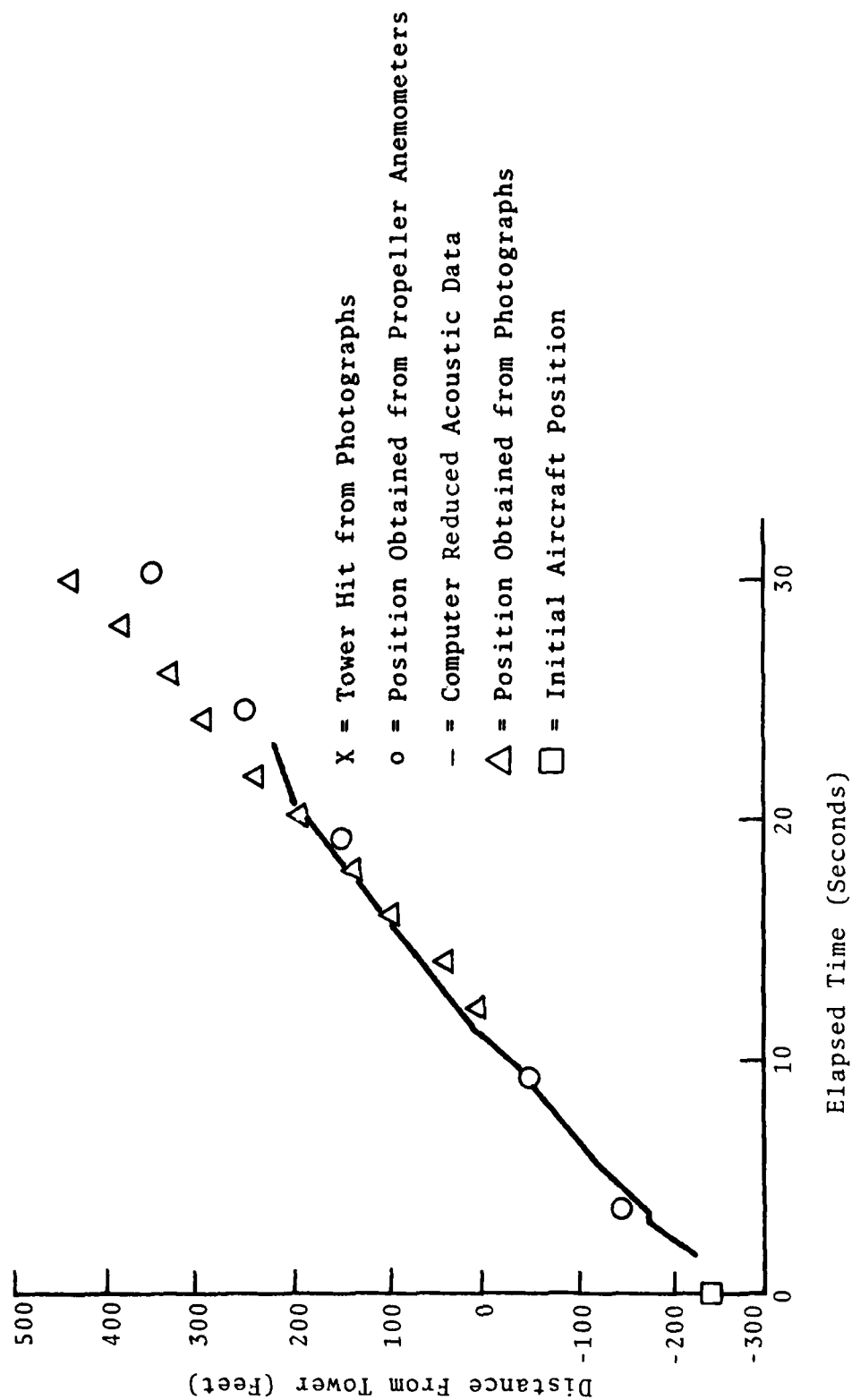


FIGURE 30. NAFEC TOWER TESTS, 9/17/72, RUN 747-44 DOWNWIND VORTEX

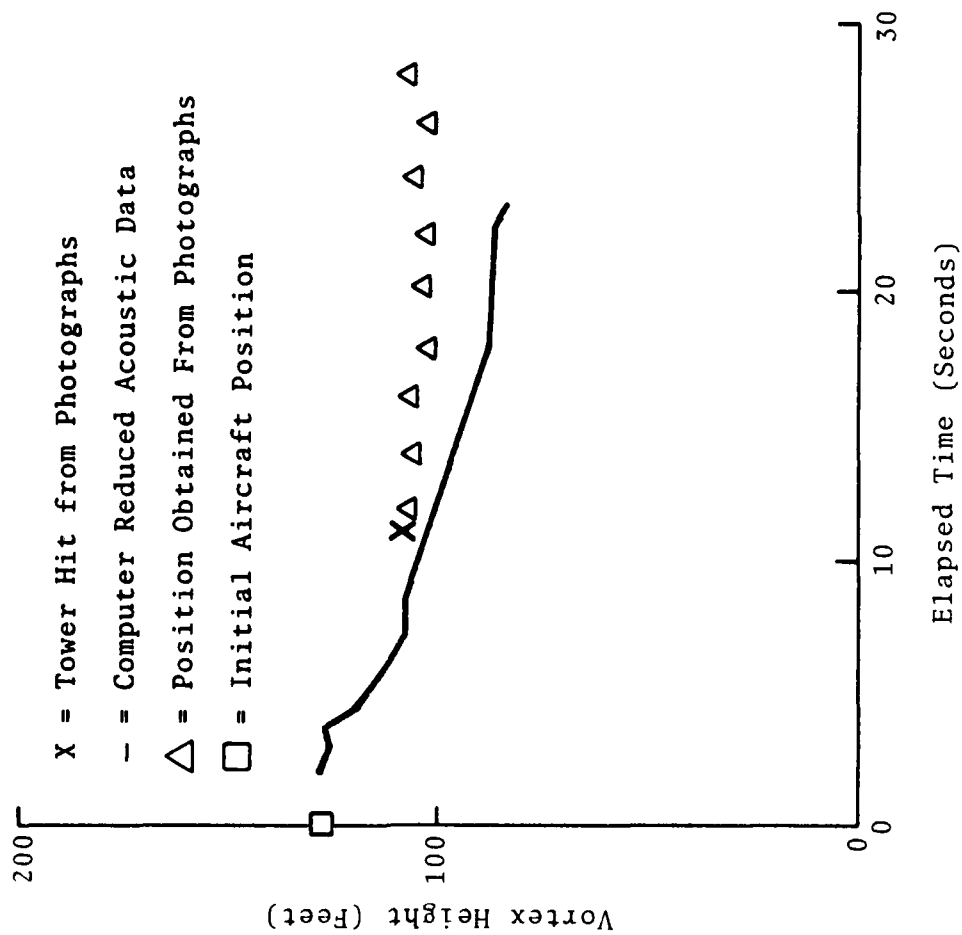


FIGURE 30. (CONCLUDED)

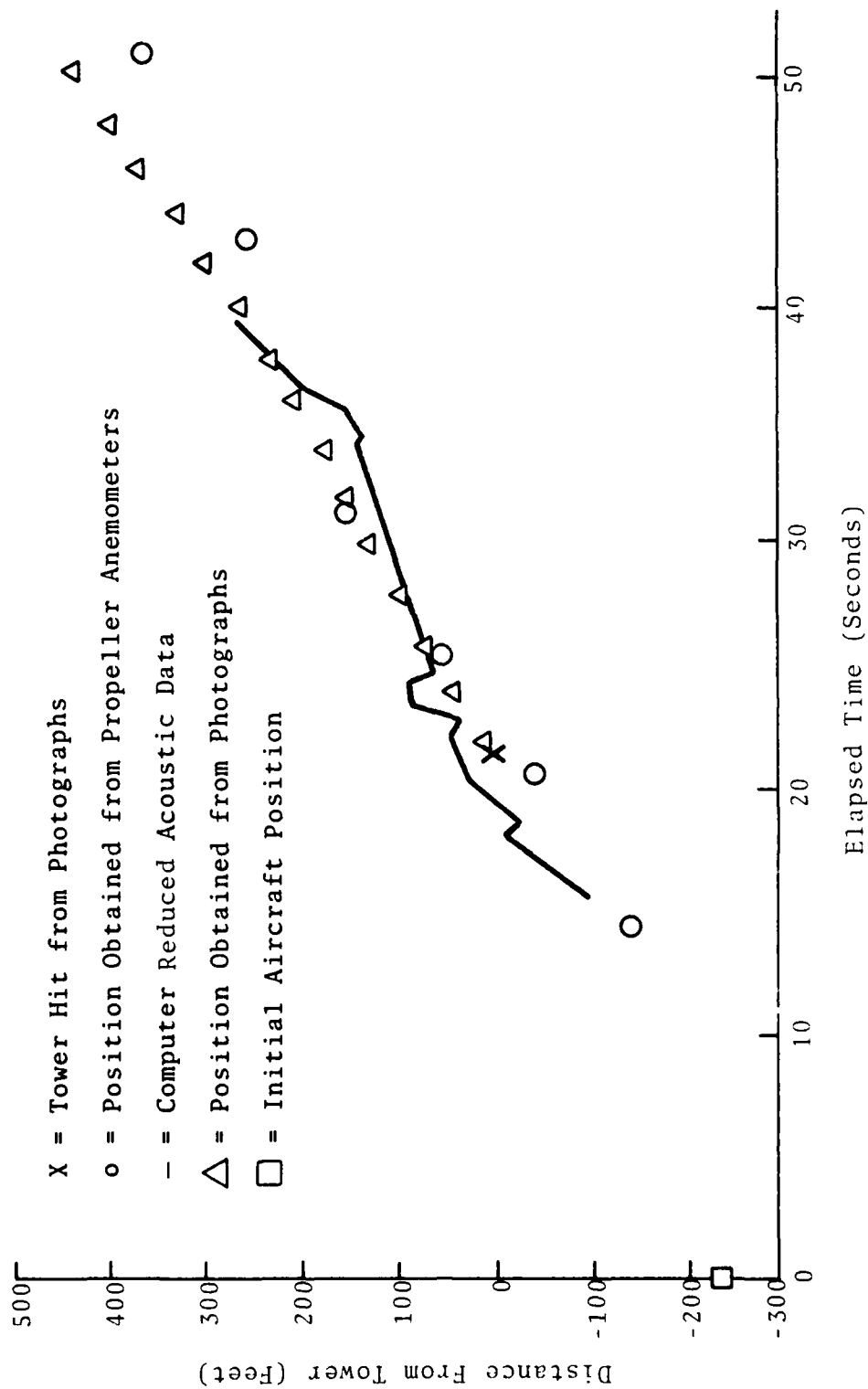


FIGURE 31. NAFEC TOWER TESTS, 9/17/72, RUN 747-44 UPWIND VORTEX

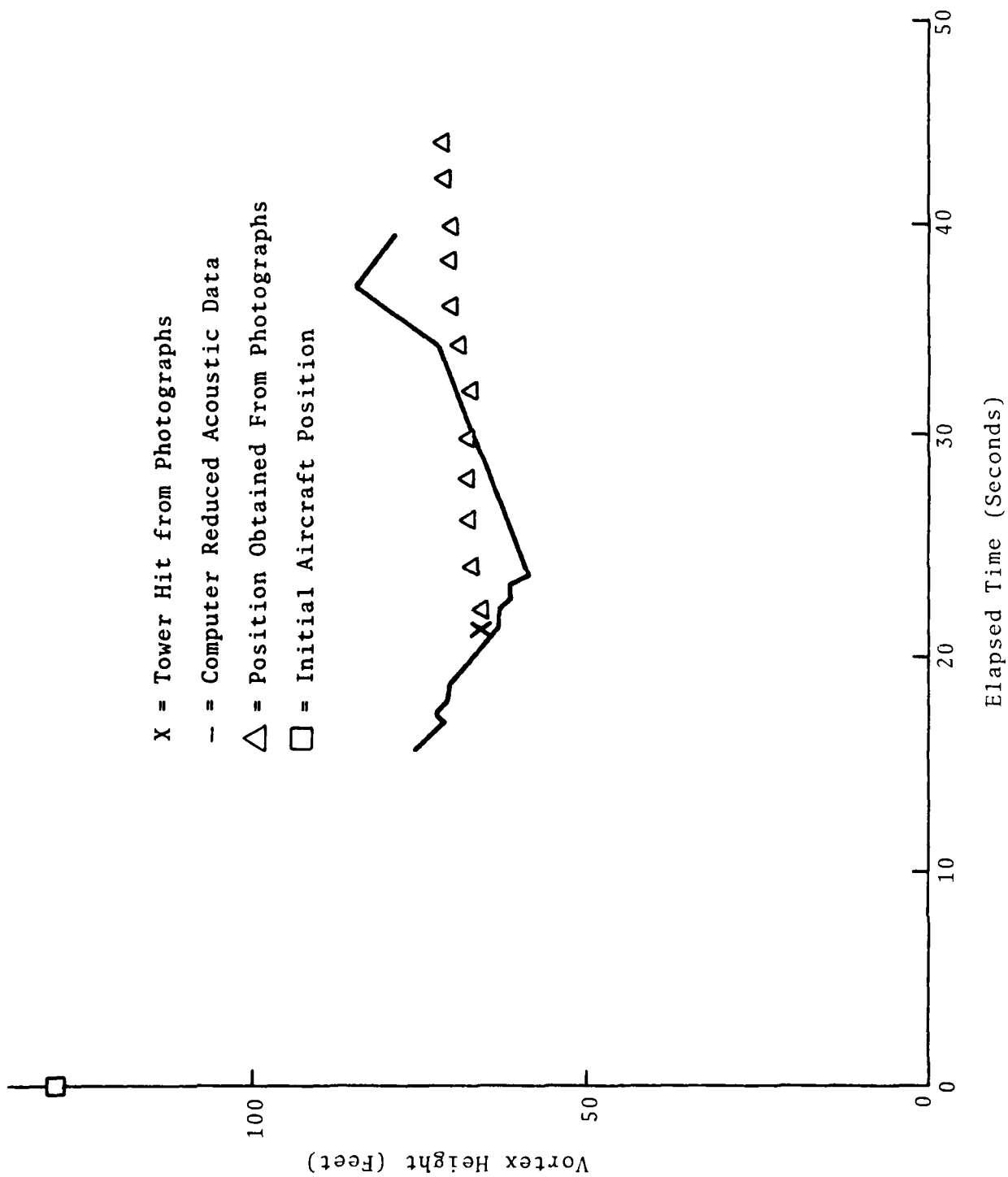


FIGURE 31. (CONCLUDED)

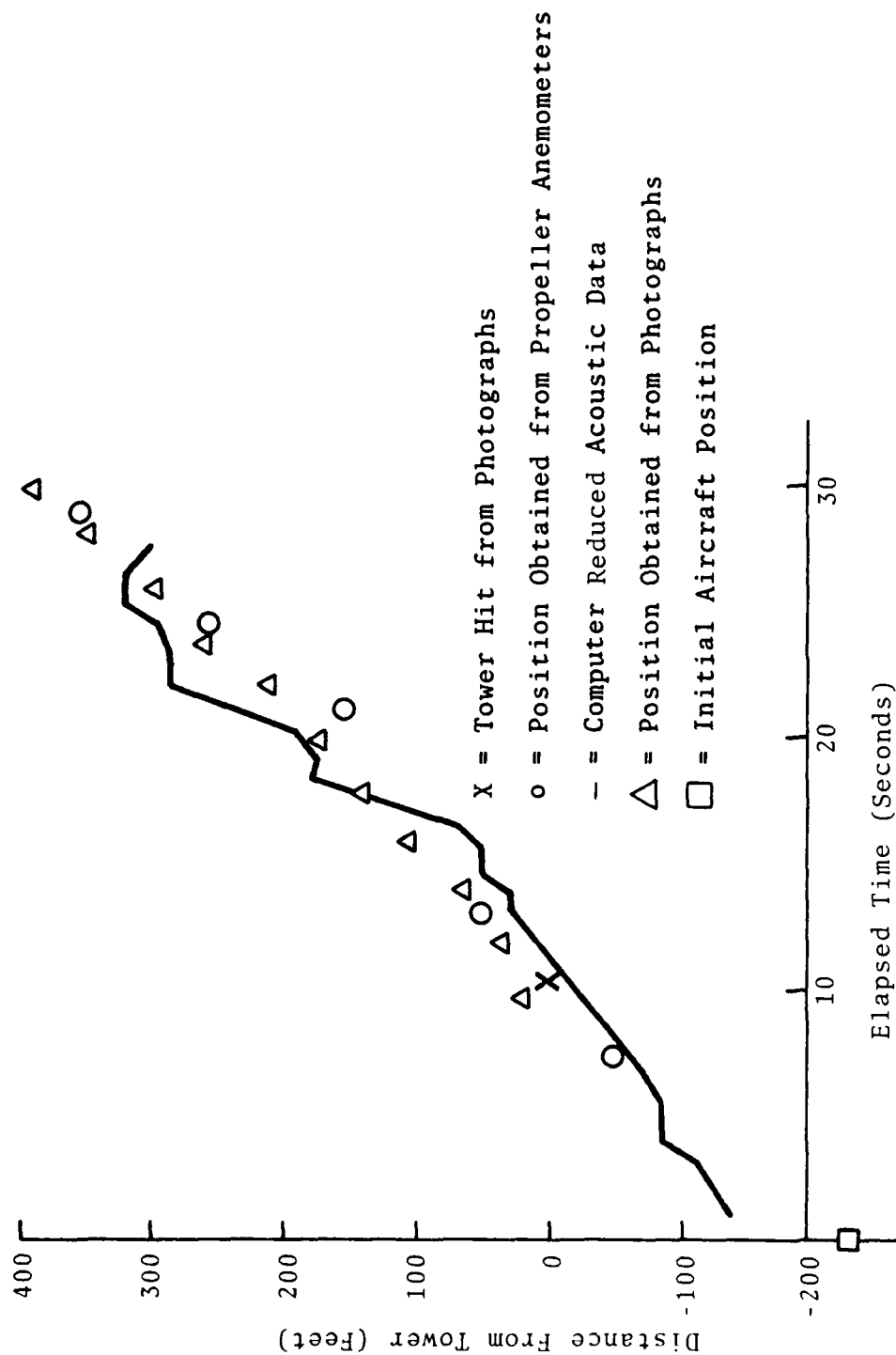


FIGURE 32. NAFEC TOWER TESTS, 9/17/72, RUN 747-45 DOWNWIND VORTEX

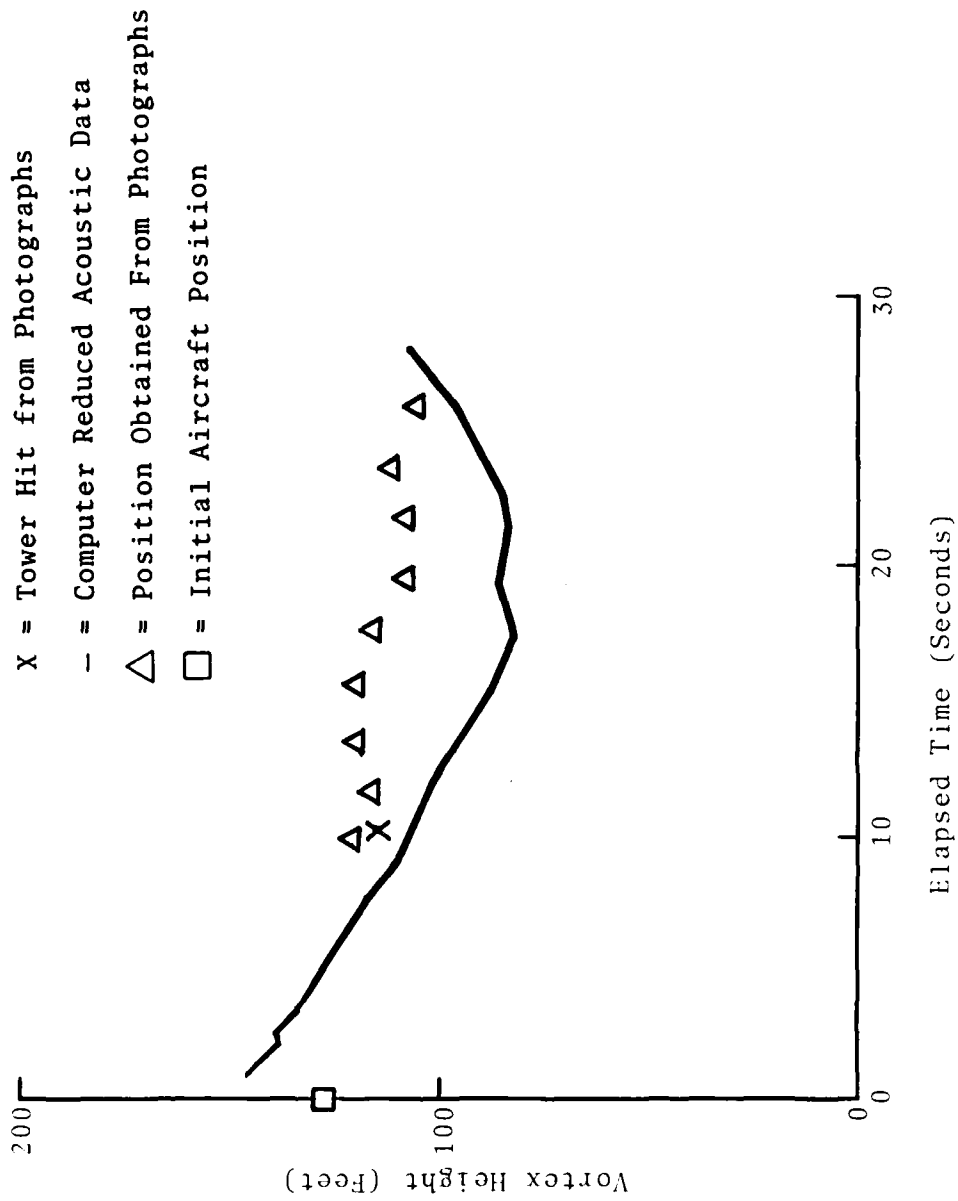


FIGURE 32. (CONCLUDED)

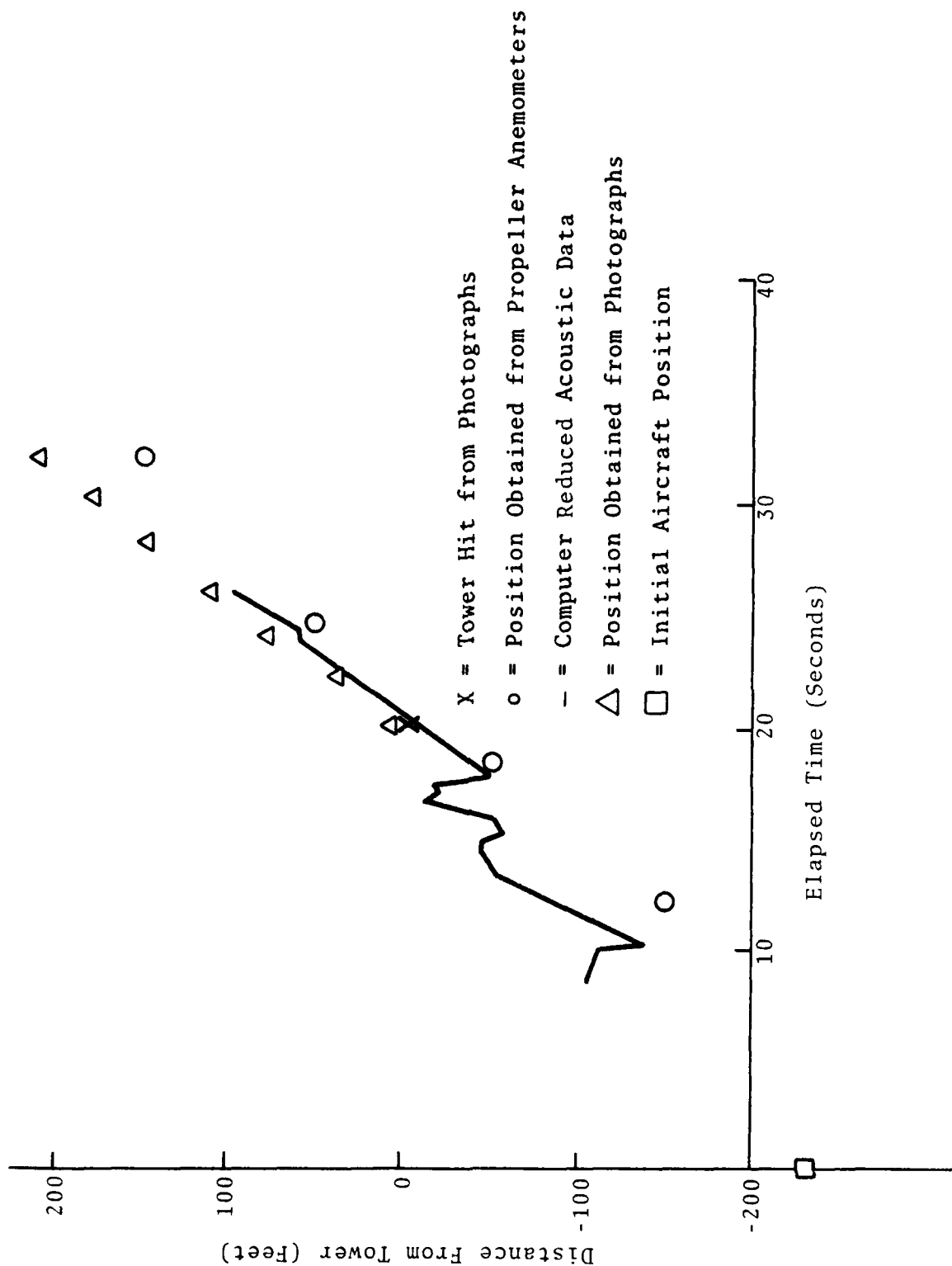


FIGURE 33. NAFEC TOWER TESTS, 9/17/72, RUN 747-45 UPWIND VORTEX

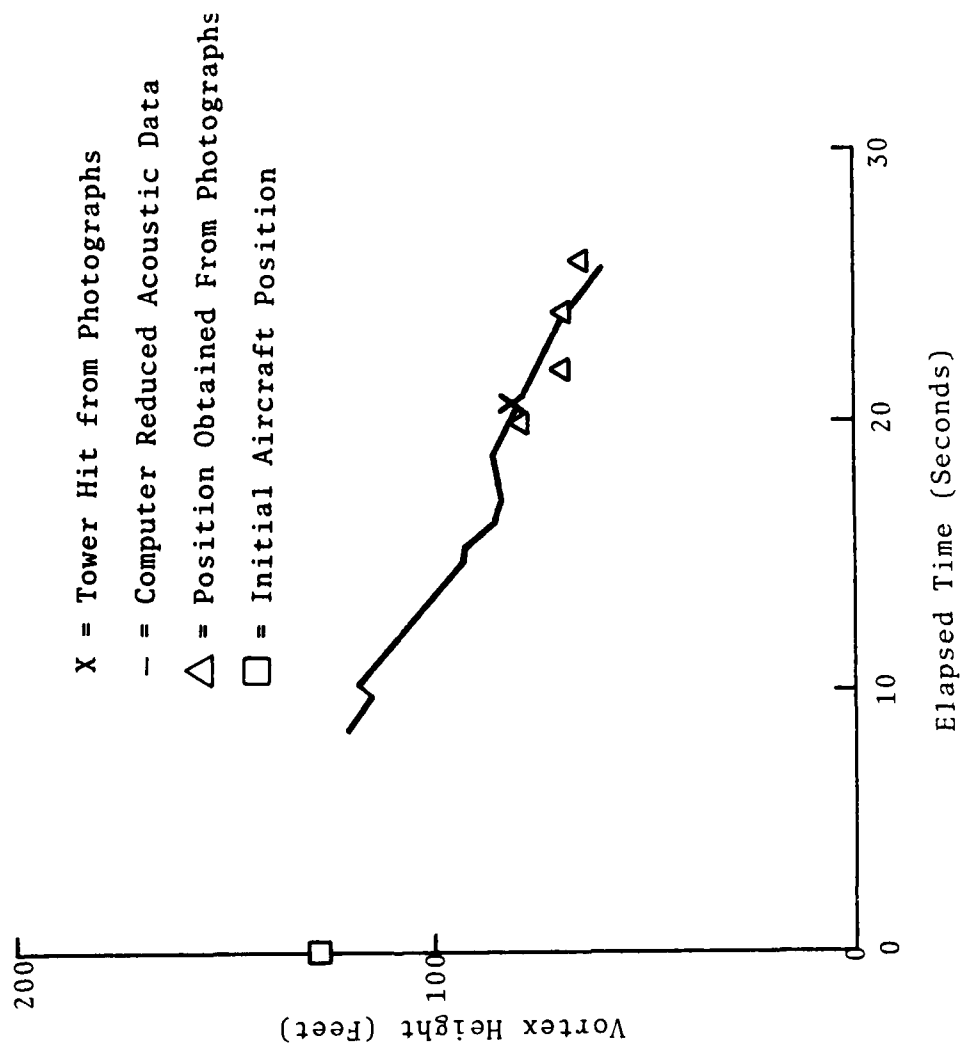


FIGURE 33. (CONCLUDED)

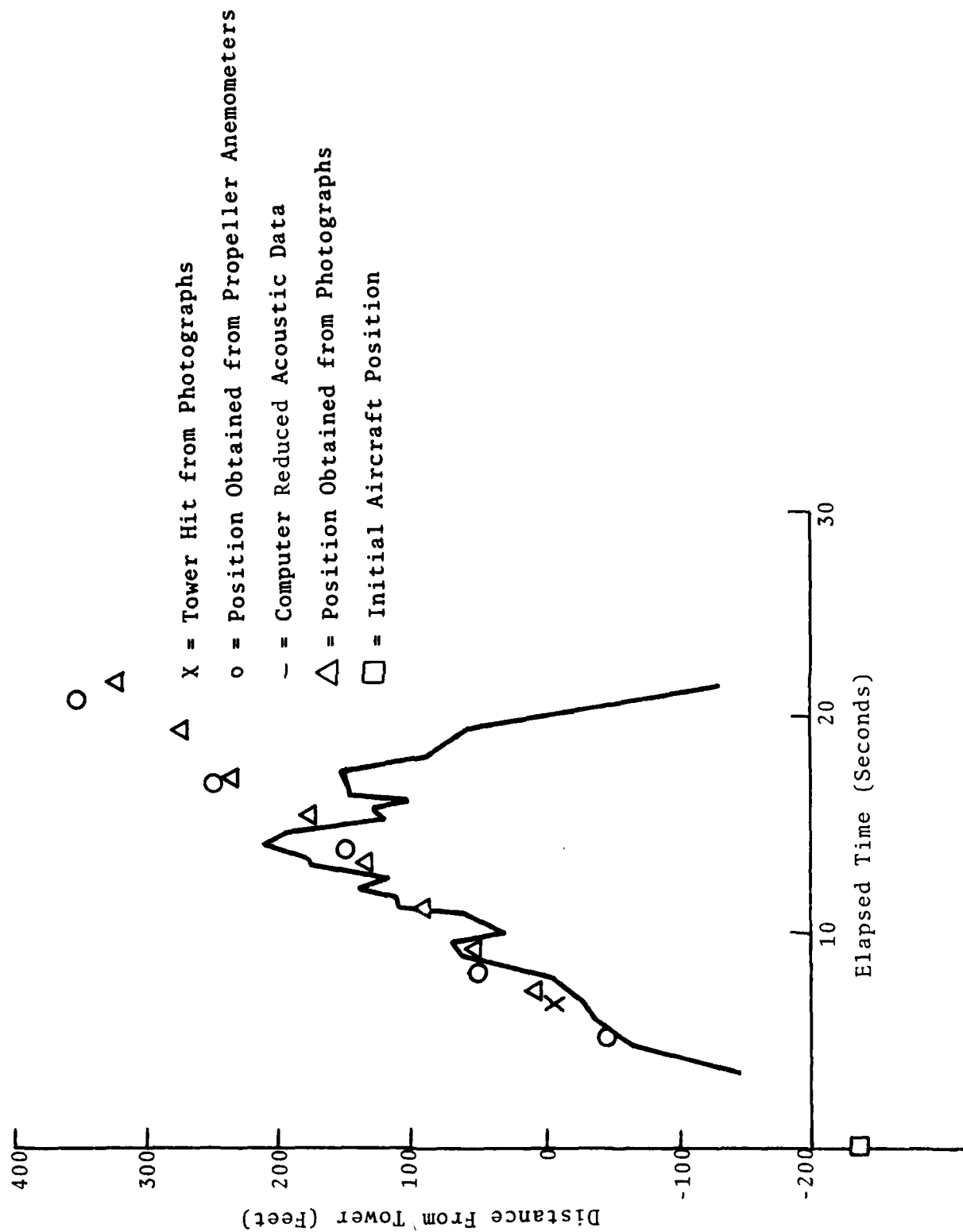
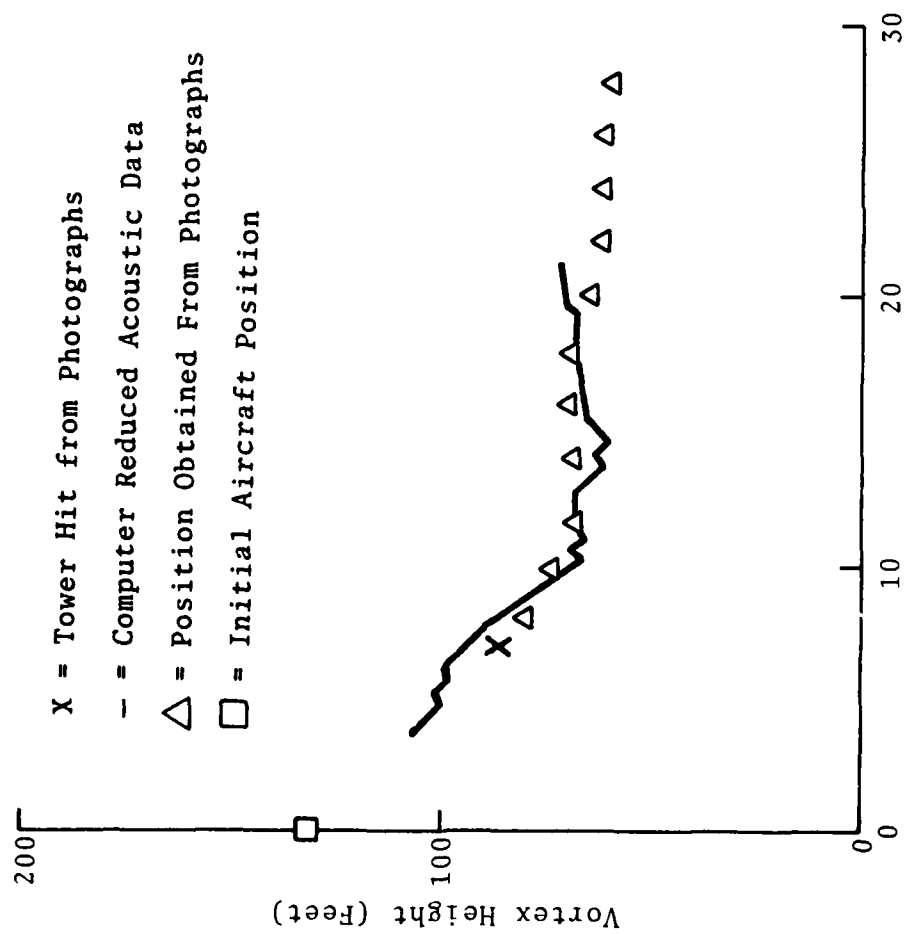


FIGURE 34. NAFEC TOWER TESTS, 9/17/72, RUN 747-48 DOWNWIND VORTEX



Elapsed Time (Seconds)

FIGURE 34. (CONCLUDED)

TABLE 5. FIGURE NUMBERS FOR VORTEX TRAJECTORY PLOTS
(PRECEDING PAGES)

Run Number	Aircraft Configuration	1st Vortex		2nd Vortex	
		x vs. t	h vs. t	x vs. t	h vs. t
727-178	L	22	22	*	*
727-180	L	23	23	*	*
727-181	L	24	24	*	*
727-182	L	25	25	+	+
747-42	TO	26	26	27	27
747-43	TO	28	28	29	29
747-44	H	30	30	31	31
747-45	H	32	32	33	33
747-48	L	34	34	*	*

Figure numbers for included results

+ = Position plot not received in time for this report

* = Insufficient data for position plot

4. DISCUSSION

4.1 ACOUSTIC SENSORS

A comparison of computer acoustograms (Figure 20) produced by AVCO with those produced manually at TSC with a Cathode Ray Tube (CRT) z-axis display indicates the following deficiencies in the AVCO analysis:

a) The sensitivity is too low since some signals which were observed on the CRT acoustogram were not present on the AVCO plot. The loss of these signals results in position calculations with high standard deviations (since the number of observed time delays is a measure of the system accuracy) and the absence of a track where there should be one.

b) The algorithms do not allow the measurement of relatively small time delays (5-10 msec.). Vortices with small acoustic scattering angles cannot be tracked.

c) The method of choosing the data points from the acoustogram is relatively unsophisticated because of the preliminary nature of the AVCO effort.

d) The accuracy with which the vortex can be located decreases greatly when the number of observed time delays is reduced, e.g., at the beginning and end of each run. (See Figure 21.)

4.2 GROUND WIND SENSORS

The agreement between the ground wind data and the photographic data is excellent. The sensors are generally more reliable for heavier aircraft - compare Figures 13 and 14 - and light ambient winds, as one would expect. The consistency of the data under the same conditions is impressive. It should be noted that the data presented here are not the best of all the data obtained. For example, the data displayed in Figure 14 are the poorest of a series of 12 consecutive runs.

A comparison of the data shown in Figures 15 and 16 illustrates the deficiencies of the pressure sensor for detecting the vortex wind when the ambient wind is perpendicular to the flight path. The first vortex passing over the sensor produces a strong signal while the second one often produces a barely discernible signal. In the absence of a parallel wind component, the wind from the second vortex subtracts directly. Since the response of the pressure sensor to the wind is quadratic, the amplitude of the signal from the first vortex tends to be much larger than that from the second. In fact, comparable signals occur only when the wind from the second vortex strongly reverses the wind direction at the sensors as in run 747-29 of Figure 15.

In the display shown in Figure 17 the vortex locations at a particular time would be assigned to the brightest (first vortex) and darkest (second vortex) sensor line. It can be seen that the vortex field of influence extends to more than one sensor at a time for B-747 vortices and 100-ft sensor spacing.

4.3 AIRCRAFT DETECTOR

The data in Figure 19 illustrate some of the capabilities of pressure sensor aircraft detectors. The arrival time of the aircraft at the baseline is easily determined. The two detectors (4 and 5) spaced 1100 ft apart along the flight path give a good indication of the aircraft speed. As the detector is displaced from the flight path, the signals decay in amplitude and increase in duration. Although not shown in these data, the same changes occur for increased aircraft altitude. These observations are consistent with the expectation that the dynamic pressure associated with the aircraft extends in all directions below the aircraft with an amplitude which decreases with distance.

Several technical problems associated with the aircraft detectors are apparent in Figure 19. The instability of detectors not using a dewar flask as the reference vessel is apparent in the 5 sec/div data of detectors 4 and 5.

Because of leaks, the time constants of the reference vessels in detectors 1 and 3 were too short to insure full response to the aircraft pressure. (Note the undershoot of detector 1.) The response of the aircraft detectors to the vortex winds can be seen by comparing the 5 sec/div data of detector 1, over which the vortices did not pass, to that of detectors 2 and 3, over which the vortices did pass. The wind response could probably be suppressed by a suitable wind screen.

5. CONCLUSIONS

The strengths and weaknesses of three types of aircraft wake vortex sensors were demonstrated and can be summarized as follows:

a) The Pulsed Acoustic Vortex sensor is useful for detecting vortices with well defined cores such as those generated from aircraft in a landing configuration with no engine in the vicinity of the outboard flap edge (so-called "clean-wing" aircraft) or almost any aircraft in a cruise configuration (almost zero flap setting). Special tests were performed with the B-707 aircraft to test this hypothesis. The aircraft executed several tower fly-bys with either its outboard port or starboard engine at idle. Observations of the smoke patterns confirmed the difference in the vortex characteristics (i.e., the vortex generated from the wing with the engine at idle had a very well-defined, high-velocity, tight core region while the vortex from the wing with engines at normal thrust had a much broader, lower-velocity, diffuse core region.) Analysis of the pulsed acoustic data confirmed that the system can reliably detect and track the tight core vortices although it has a great deal of difficulty detecting the vortices of the diffuse core type. Vortex detection with this system becomes difficult when the core region is less well-defined as when the vortex ages or when a landing aircraft has an engine located close to the major lift discontinuity, the outside edge of the outboard flap. These two factors severely limit the use of this sensor for large-scale data collection on vortex behavior.

A series of special tests with the B-727 aircraft were performed to test the systems capability to detect and track vortices at higher altitudes. Using the specially designed, extra large, 2500 foot (758 m) acoustic system baseline, it was determined that the system was capable of tracking vortices up to an altitude of approximately 800 feet (242 m).

b) Pressure sensors can be used to detect aircraft vortices and have the advantage of having no moving parts and therefore

very little maintenance. Their nonlinear response, however, limits their use to detecting only the strongest vortices under very low ambient wind conditions.

c) The propeller anemometer is a very reliable vortex sensor. Comparison of the data obtained with the propeller anemometer arrays to that obtained from the photographs of actual vortex location demonstrates the excellent accuracy and ability of this sensor to detect and track aircraft vortices. The sensor does, however, have two limitations. Because of its relatively complex system of moving parts, its performance has been observed to degrade under certain meteorological conditions. (The propeller motion can be stopped in freezing rain, and dirt and dust in the atmosphere can lead to bearing damage and the necessity of relatively frequent maintenance.) Also the propeller anemometer system yields very little information on either the vortex height or strength. It has been empirically determined that in relatively low winds the system will continue to indicate the presence of a vortex for a significant time after the vortex has decayed to an insignificant level.

It can be seen from the data presented in Figures 22-34 that the vortices are almost always detected first by the pulsed acoustic system. This is due to the insensitivity of the propeller anemometer system for detecting vortices at relatively high altitudes. The propeller anemometer system, however, generally tracks vortices over longer times and distances. This is due to the inability of the pulsed acoustic system to detect and track vortices after the vortex core has become relatively diffuse. Although it is not shown in these figures, it is common for the propeller anemometer system to track vortices after tracking with the photographs has ceased. This is due to the propeller anemometer's high sensitivity in detecting very low-level winds. It should be pointed out that this is not always a virtue since the detected vortex may be only a very weak remnant and possibly should not be considered as a vortex in the usual sense. Of the three sensors only the propeller anemometer appears to be a serious candidate as

a vortex sensor for collecting large quantities of data on vortex behavior for actual aircraft operations.

Some of the data collected during these tests were used to compare to tracks predicted by models of vortex behavior. Very good agreement between predicted and actual vortex behavior was obtained and is presented in Reference 4.

6. REFERENCES

1. D. Burnham, M. Gorstein, J. Hallock, R. Kodis, I. McWilliams, T. Sullivan, "Aircraft Wake Vortex Sensing Systems," Report Nos. DOT-TSC-FAA-72-13/AD-744-864 (June 1971).
2. D. Burnham, J. Hallock, R. Kodis, T. Sullivan, "Vortex Sensing Tests at NAFEC," Report Nos. DOT-TSC-FAA-72-1/AD-749-908 (January 1972).
3. T. Sullivan, D. Burnham, R. Kodis, "Vortex Sensing Tests at Logan and Kennedy Airports," Report Nos. DOT-TSC-FAA-72-25/FAA-RD-72-141/AD-753-849 (December 1972).
4. M.R. Brashears and J.N. Hallock, "Aircraft Wake Vortex Transport Model," J. Aircraft, 11 (5), 265-272 (May 1974).

APPENDIX -- ANALYSIS OF PHOTOGRAPHIC TRACKING DATA

The photographs of tower smoke give the apparent location of the vortex over the baseline, which is calibrated in the horizontal direction by means of signs located at the positions of the ground level sensors. (See Figure 1 and Tables 1 and 2.) The actual position of the vortex over the baseline depends upon the relative location of the baseline with respect to the smoke tower, the direction of the wind, and the angle of the vortex with respect to the baseline. The geometrical analysis of these corrections is based on Figure A-1. The smoke tower is the origin of the coordinate system. The smoke blows downwind from the tower along line #1:

$$\text{Line \#1: } y = x \tan \theta \quad (\text{A1})$$

The angle of the wind, θ , is taken from the sensor at the 140 ft. level of the smoke tower. The measurement of the photograph determines the apparent position (X_1 , $-A$, H_1) of the vortex core over the baseline ($y = -A$). The apparent height, H_1 , of the vortex core is determined by using the 140 ft tower as the scale of height. Line 2 passes through point #1 and the camera site (D , $-L$, C).

$$\text{Line \#2: } x = c_1 y + c_2 \quad (\text{A2})$$

$$c_1 = (X_1 - D) / (L - A) \quad (\text{A3})$$

$$c_2 = D + LC_1. \quad (\text{A4})$$

The location, point #2 (X_2 , Y_2 , H_2), of the vortex core in the smoke is given by the intersection of lines #1 and #2:

$$X_2 = C_2 (1 - C_1 \tan \theta)^{-1} \quad (\text{A5})$$

$$Y_2 = X_2 \tan \theta. \quad (\text{A6})$$

The actual height H_1 is given by:

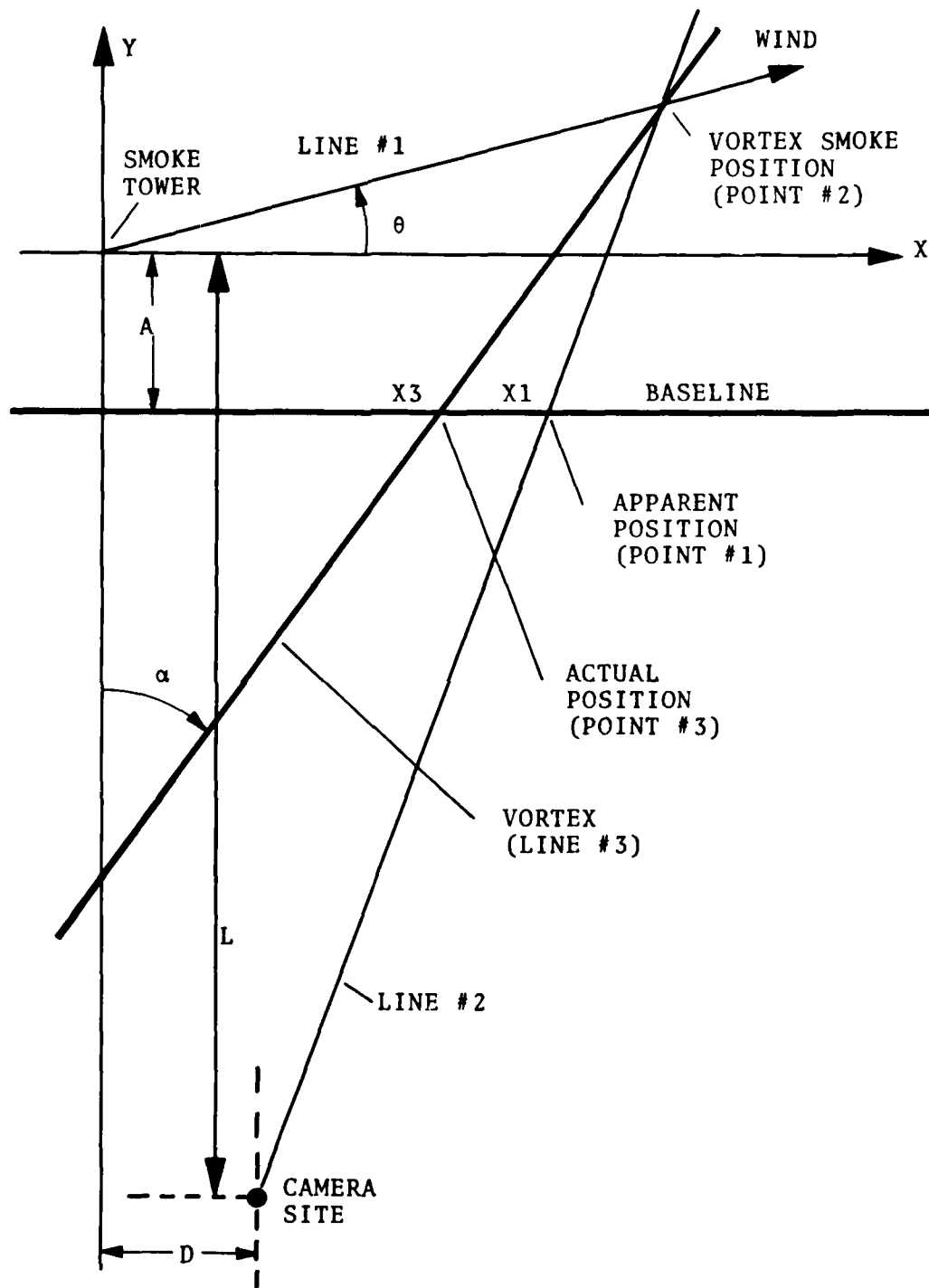


FIGURE A1. GEOMETRICAL ANALYSIS OF VORTEX LOCATION

$$H1 = H2[(X2-D)^2 + (Y2+L)^2/(D^2+L^2)]^{1/2}. \quad (A7)$$

The vortex core, line #3, passes through point #2 at angle α , which is simply the magnetic heading of the aircraft, taken from the pilot data sheets.

$$\text{Line 3: } x=y \tan \alpha + C_3 \quad (A8)$$

$$C_3 = X2 - Y2 \tan \alpha. \quad (A9)$$

The actual location, point #3 ($X3$, $-A$, $H3$), of the vortex core over the baseline is given by the intersection of line #3 with the baseline:

$$X3 = -A \tan \alpha + C_3. \quad (A10)$$

If the vortex core is horizontal, the height over the baseline is the same as that at the smoke:

$$H3 = H2 \quad (A11)$$

$X3$ and $H3$ are thus obtained from $A1$, $H1$, θ , α , A , D and L by means of equations $A10$, $A9$, $A6$, $A5$, $A4$, $A3$ and equations $A11$, $A7$ respectively.

Errors in this procedure can be introduced by inaccurately measured values of θ and α , especially θ . Under the conditions of the experiments, $L \gg A$, $L \gg X1$, the error is minimized for $|\theta| \ll 1$ and $|\alpha| \ll 1$, i.e., the wind blowing down the baseline and the aircraft perpendicular to the baseline. However, for large values of $|\theta|$ significant errors may occur, especially for large values of $X1$.